The late Pleistocene-early Holocene rails (Gruiformes: Rallidae) of Laguna de Tagua Tagua Formation, central Chile, with the description of a new extinct giant coot

Jhonatan Alarcón-Muñoz [a,b,c,d,*], Rafael Labarca [b,e], Sergio Soto-Acuña [a,b,d]

[a] *Red Paleontológica U-Chile, Laboratorio de Ontogenia y Filogenia, Facultad de Ciencias, Universidad de Chile, Las Palmeras, 3425, Santiago, Chile*
[b] *Corporación Laguna de Taguatagua, Av. Libertador Bernardo O'Higgins 351, Santiago, Chile*
[c] *Laboratorio de Zoología de Vertebrados, Departamento de Ciencias Ecológicas, Facultad de Ciencias, Universidad de Chile, Las Palmeras, 3425, Santiago, Chile*
[d] *Kaytreng Consultores. José Domingo Cañas 1640, DP, 1502, Ñuñoa, Santiago, Chile*
[e] *Escuela de Arqueología and Transdisciplinary Center for Quaternary Research (TAQUACH), Universidad Austral de Chile, Puerto Montt, Chile*

ARTICLE INFO

ABSTRACT

Rallidae, which includes coots, crakes and moorhens, is one of the most speciose families among the Gruiformes. This family exhibits a pattern of diversification that has involved significant episodes of regional expansion and speciation resulting in the presence of members of this group in every continent with the exception of Antarctica. In this work, we describe the diversity of fossil rallids from late Pleistocene-early Holocene deposits of the Laguna de Tagua Tagua Formation located in central Chile. We report the presence of the extant taxa, *Fulica armillata*, *Fulica rufifrons*, *Fulica* cf. *F. rufifrons*, *Fulica* cf. *F. ardesiaca* and *Pardirallus sanguinolentus,* and also identify a large new extinct coot, *Fulica montanei* sp. nov. represented by three left tarsometatarsi. *Fulica montanei* corresponds to the first extinct rallid recorded in the Quaternary of South America. The most remarkable feature of the tarsometatarsus of *Fulica montanei* is their large size, which falls in the range of the extant Andean species *Fulica cornuta* and the extinct *Fulica prisca* from New Zealand. An autapomorphic combination of characters observed in the tarsometatarsi also supports the erection of a new species. These rails coexisted with extinct megafauna, as well as small and medium-sized vertebrates and, presumably, with humans, constituting a faunal assemblage with no analogous today. *Fulica montanei* probably became extinct during the late Pleistocene-early Holocene.

1. Introduction

The family Rallidae includes small to medium-sized aquatic or semi-aquatic birds commonly known as coots, crakes and moorhens (Taylor, 2010; Winkler et al., 2020). The group includes around 135–143 currently recognized species grouped within 33–40 genera and representing about 1.3% of current known birds (Taylor, 1998; Houde, 2009; Clements et al., 2012). The family exhibits a diversification pattern that involved several episodes of regional expansion and speciation probably since the Eocene (García-R et al., 2014, García-R et al., 2020). As a result, Rallidae is represented in every habitable continent at present (García-R et al., 2014). This process of diversification was partially aided by the great dispersal ability of these birds and by their capability to exploit different ecological opportunities (García-R et al., 2014). An important portion of the rail's fossil record comes from islands (i.e East

Pacific, Caribbean, Madagascar, Mediterranean) suggesting that insular isolation stimulated rapid and repeated speciation processes, which usually implied the loss of flight ability (Olson, 1973; Ripley, 1977; Holdaway et al., 2001; Alcover et al., 2005; Kirchman and Steadman, 2005, 2007; Mcminn et al., 2005; Gill et al., 2010; Worthy and Boles, 2011; Mather et al., 2018; Hume, 2019; Hume and Martill, 2019, among others).

In South America the rallid fossil record is scarce and comes mostly from Quaternary deposits. Older putative rallids (Alvarenga, 1988; Noriega, 1995) (i.e Oligocene-Pliocene), have not been formally described (Tambussi and Degrange (2013)) or taxa erected have been subsequently reassigned to other families (Mourer-Chauviré, 2000; Noriega and Agnolin, 2008). With respect to the Quaternary record, Olson (1977) questioned the validity of the species *Euryonotus brachypterus* and *Euryonotus argentinus* described by Mercerat in 1897 from

the late Pleistocene of Buenos Aires, although, the same author suggested the presence of an extinct flightless rail from the island of Fernando de Noronha in Brazil without offering a formal description (Olson, 1977, 1981). Other findings come from scattered localities in Perú, Ecuador, Argentina, Bolivia and Chile, from which only extant forms have been recognized (Campbell, 1979; Tonni and Laza, 1980; Humphrey et al., 1993; Vezzosi et al., 2010; Cenizo et al., 2015).

In Chile, the rallids are currently represented by the genera *Fulica*, *Gallinula*, *Laterallus*, *Pardirallus*, *Porzana*, *Porphyrio*, *Porphyriops* and *Rallus*, counting at least 14 extant species, some of them resident while others reported as occasional sightings (Couve et al., 2016; Martínez-Piña and González-Cifuentes, 2017). Among these, *Fulica* is the most speciose genus, with six species (Couve et al., 2016; Martínez-Piña

and González-Cifuentes, 2017). Three species inhabit ecosystems in the Andean altiplano (~17°5′-27°S, ~3000 msnm): the slate-colored coot (*Fulica ardesiaca* Tschudi), the horned coot (*Fulica cornuta* Bonaparte) and giant coot (*Fulica gigantea* Eydoux and Soulyet) (Couve et al., 2016; Martínez-Piña and González-Cifuentes, 2017), while the remaining rallids are commonly found in low-altitude areas ranging from the semiarid valleys in north-central Chile (~27°S) to southern Patagonia (53–54°S). The only exception to this is the common gallinule (*Gallinula galeata* Lichtenstein) confined to low-altitude freshwater bodies in the northern portion of the country (~17°5′-21°S) (Couve et al., 2016).

In the present contribution we describe the diversity of fossil rails from late Pleistocene-early Holocene deposits of the Laguna de Tagua Tagua Formation, located in central Chile (Fig. 1). Additionally, we

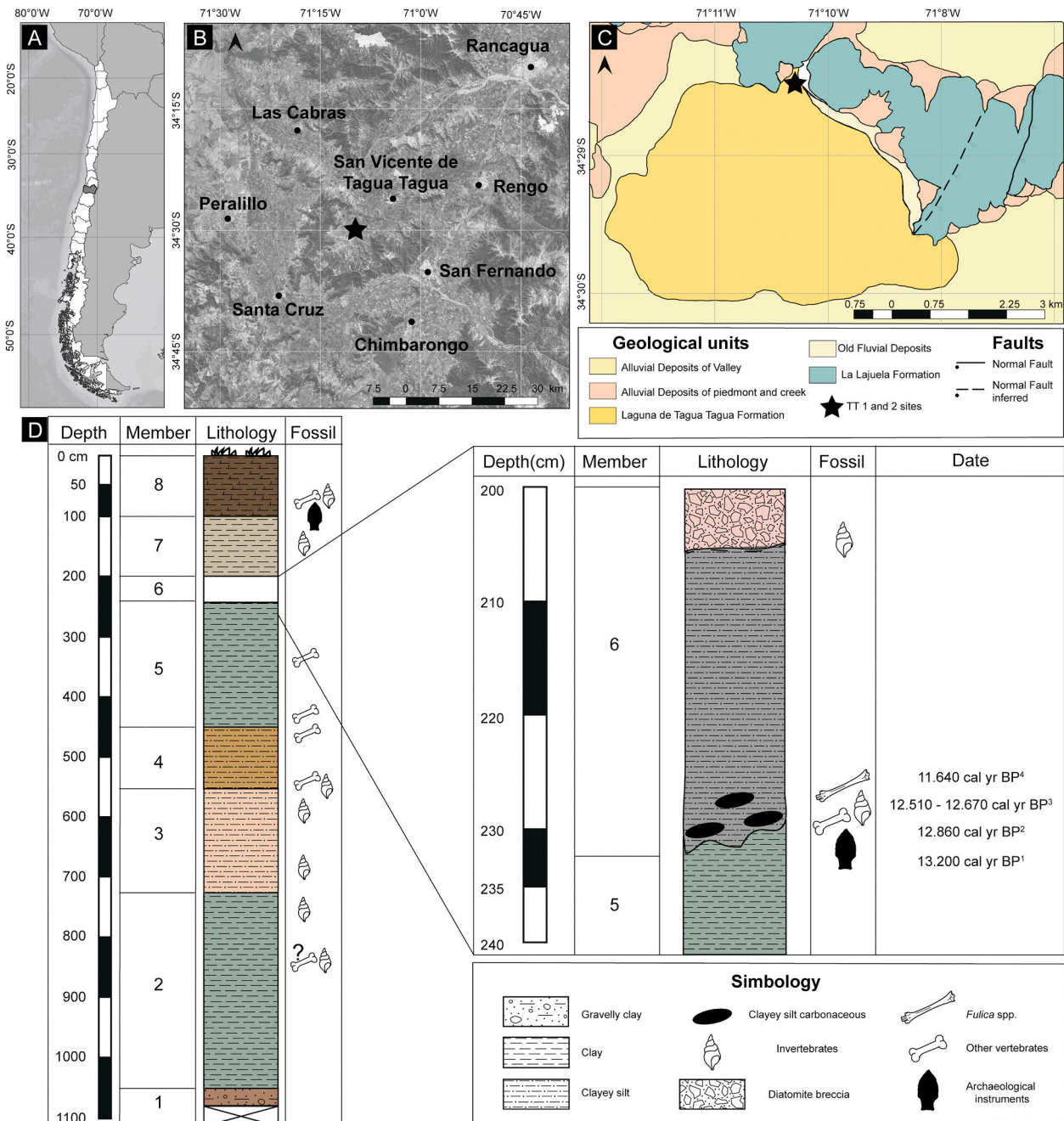**Fig. 1.** Geographic location of the study area and geological setting. (**A**) Geographic location in South American context. (**B**) Geographic location in regional context. (**C**) Geological setting of Laguna de Tagua Tagua area. (**D**) Scheme of the studied stratigraphic section of Laguna de Tagua Tagua Formation and detail of the Pleistocene-Holocene transition. Modified from Labarca et al. (2020).

report a new large species, *Fulica montanei* sp. nov. based on the description of three left tarsometatarsi. *Fulica montanei* corresponds to the first Quaternary extinct rallid recorded in South America. The findings presented here help to improve our knowledge about the late-Pleistocene-early Holocene diversity of coots in South America.

2. Materials and methods

In this work we describe twenty-two appendicular bones of rallids, all of them found disarticulated during excavations led by the archaeologist Lautaro Núñez in 1990 in Laguna de Tagua Tagua. These fossil specimens are housed in the Museo Nacional de Historia Natural de Santiago de Chile (MNHNCL SGO.PV.).

Quantitative and qualitative comparisons were made with extant and extinct coots from the following collections: Museo de Historia Natural de Santiago de Chile (MNHNCL), Laboratorio de Zoología de Vertebrados, Universidad de Chile, (UCHZV), Museo de La Plata, Argentina (MLP), Museo Argentino de Ciencias Naturales Bernardino Rivadavia, Argentina (MACN), Museum of Natural Science, Louisiana State University, United States (LSU), Florida Museum of Natural History, United States (FLMNH), Canterbury Museum, New Zealand (CMNZ), Museum of New Zealand Te Papa Tongarewa, New Zealand (DM), Marcos Cenizo's personal collection (MMC) and Douglas Jackson's personal collection (DJS). The tarsometatarsi of the following specimens were used: *Porphyriops melanops* (UCHZV-535), *Pardirallus sanguinolentus* (UCHZV-408), *Fulica gigantea* (LSU 83948, MACN-Or-2318a; UCHZV-377), *Fulica cornuta* (FLMNH UF39765), *Fulica ardesiaca* (LSU 51035, LSU 157352, UCHZV-322), *Fulica armillata* (MNHNCL/AVE 551, MLP-PV-OR 49, MACN-Or 2306 B, MACN-Or 37965, MACN-Or 68679, MACN-Or 68703, MMC110, MMC 125, DJS-227, UCHZV-333, UCHZV-515), *Fulica rufifrons* (MNHNCL/AVE 002, MACN-Or 37966, MACN-Or 54815, MACN-Or 54816, MACN-Or 54835, MMC 080, MMC 082, MMC 091, UCHZV-320, UCHZV-542), *Fulica leucoptera* (LSU 125646, LSU 125647, MLP-PV-OR 50, MLP-PV-OR 813, MLP-PV-OR 816, MACN-Or 1575 A, MMC 019, MMC 123, MMC 124, MMC 154, MMC 296), *Fulica atra* (LSU 152973), *Fulica americana* (LSU 73152, LSU 73153, LSU 112372, LSU 118613), *Fulica cristata* (LSU 118924) and with the fossil species *Fulica chathamensis* (CMNZ 7582,1, 7582,2, 7582,3, 7582,4, 7582,5, 7582,6, 7582,7, 7582,8, 7582,9, 11008) and *Fulica prisca* (DM380, CMNZ 45428,2, 5589, 9759, 10710, 11598, 11653, 12827, 12831, 13550).

Osteological terminology follows Baumel and Witmer (1993). For the description of the orientation of structures in the coracoid, the proposal of Livezey and Zusi (2006) was followed. Additionally, for the description of the hypotarsus, the proposals in Mayr (2004, 2015 and 2019) were followed. For the description of hypotarsal crests, we use the terms "lateral, intermediate and medial hypotarsal crest" since the nomenclature used for these structures in Baumel and Witmer (1993) does not necessarily reflect the homology of these crests (Mayr, 2015, 2019). Measurements were taken using digital calipers with 0.01 mm increments following von den Driesch (1976).

Univariate and multivariate statistical analyses were performed to explore size differences among different specimens of *Fulica*. The former included scatter plots considering GL and Bp. The multivariate statistics included principal component analysis (PCA) considering GL, Bp, SC and Bd measurements. Metrical data was taken from Table 1.

3. Geographic and geological setting

Rallidae fossil specimens come from the Laguna de Tagua Tagua Formation (LTTF), described and defined in the former Laguna de Tagua Tagua (Tagua Tagua lake), located in the oriental margin of the Coastal Range of central Chile (34°29′S; 71°10′W) (Fig. 1A–D). The LTTF consists of a 12,6 m thick deposit of semi-consolidated lacustrine sediments, such as clay and silt, unconformably overlaying to tuff layers (Varela, 1976). Extrapolated sedimentation rates and radiocarbon dates suggest

Table 1

Metatarsi measurements (in mm) of different *Fulica* species. Measurements according to von den Driesch (1976).

Repository Code	Taxa	GL	Bp	SC	Bd
SGO.PV.22320	*F. montanei*	80,69	13,49	5,23	13,74
SGO.PV.22321	*F. montanei*	77,50	–	5,03	–
SGO.PV23240	*F. montanei*	–	–	–	12,25
SGO.PV.27789	*F. armillata*	73,25	10,82	4,60	10,9
SGO.PV.23236	*F. armillata*	63,25	10,43	4,23	10,87
SGO.PV.22239	*F. armillata*	–	–	4,47	10,69
SGO.PV.23334	*F. armillata*	66,74	11,22	4,66	11,71
LSU 83948	*F. gigantea*	95,0	15,7	5,7	15,2
MACN-Or 2318a	*F. gigantea*	99,6	16,37	6,8	16,21
FLMNH UF39765	*F. cornuta*	79,9	13,8	4,7	14,2
UCHZV-322	*F. ardesiaca*	64,1	10,1	4,5	10,5
MLP-PV-OR 49	*F. armillata*	70,5	11,07	4,9	11,43
MACN-Or 68703	*F. armillata*	63,54	10,33	4,16	10,68
MACN-Or 68679	*F. armillata*	69,3	10,85	4,94	11,15
MACN-Or 37965	*F. armillata*	64,72	11,38	5,1	11,36
MACN-Or 2306 B	*F. armillata*	68,46	11,28	5,04	11,26
MMC 125	*F. armillata*	70,1	11,59	4,52	11,87
MMC 295	*F. armillata*	66,28	10,43	3,69	9,91
MMC 110	*F. armillata*	64,63	9,98	4,05	10,16
DJS-56	*F. armillata*	60,75	8,94	4,32	9,74
DJS-227	*F. armillata*	64,94	10,5	4,4	10,33
MNHN-551	*F. armillata*	63,47	11,02	4,4	11.4
MACN-Or 54815	*F. rufifrons*	57,21	8,82	3,96	10,12
MACN-Or 37966	*F. rufifrons*	59,91	9,54	4,65	9,56
MACN-Or 54816	*F. rufifrons*	57,77	8,64	4,14	8,86
MACN-Or 54835	*F. rufifrons*	55,73	8,38	3,69	8,83
MMC 091	*F. rufifrons*	59,88	8,82	3,92	8,97
MMC 082	*F. rufifrons*	58,87	8,88	4,07	9,08
MMC 080	*F. rufifrons*	57,94	8,63	3,76	9,25
MNHN-002	*F. rufifrons*	62,62	9,55	4,52	10,82
MLP-PV-OR 50	*F. leucoptera*	57,93	9,09	4,13	9,4
MLP-PV-OR 813	*F. leucoptera*	54,09	8,23	4,01	8,44
MLP-PV-OR 816	*F. leucoptera*	53,46	8,91	3,94	9,01
MACN-Or 1575a	*F. leucoptera*	55,08	8,2	3,55	8,55
MMC 296	*F. leucoptera*	57,95	9,74	3,97	9,9
MMC 154	*F. leucoptera*	60,27	9,64	3,81	9,88
MMC 124	*F. leucoptera*	60,18	9,02	3,88	9,47
MMC 019	*F. leucoptera*	55,67	8,5	3,73	8,93
MMC 123	*F. leucoptera*	57,56	9,23	3,67	9,07
LSU 125646	*F. leucoptera*	58,7	9,4	3,7	9,6
LSU 125647	*F. leucoptera*	51,1	8,2	3,4	8,2
LSU 152973	*F. atra*	57,4	9,0	3,4	9,1
LSU 73152	*F. americana*	55,3	8,6	3,7	8,5
LSU 112372	*F. americana*	57,8	8,8	3,8	8,9
LSU 118924	*F. cristata*	62,0	9,9	4,0	9,4
CMNZ 7582,1	*F. chathamensis*	95,1	15,8	7,5	16,3
CMNZ 7582,2	*F. chathamensis*	85,4	15,2	6,5	15,3
CMNZ 7582,3	*F. chathamensis*	91,4	15,9	6,6	15,6
CMNZ 7582,6	*F. chathamensis*	88,6	15,5	7	15,7
CMNZ 11008	*F. chathamensis*	100,1	16	6,9	16,3
CMNZ 13550	*F. prisca*	85,7	13,1	5,8	14,2
CMNZ 12831	*F. prisca*	80,4	13,77	5,5	13,1
CMNZ 11598	*F. prisca*	77,1	13,2	5,3	13,1
CMNZ 45428,1	*F. prisca*	89,8	25,2	7,2	16,1
CMNZ 45428,2	*F. prisca*	85	14,2	6,3	14,3
CMNZ 12827	*F. prisca*	87	14,7	6,7	16,2
CMNZ 11653	*F. prisca*	95,5	14,9	7,1	16,7
CMNZ 10710	*F. prisca*	87,4	13,7	5,7	14,3
CMNZ 9759	*F. prisca*	81	13,4	5,5	13,6
CMNZ 5589	*F. prisca*	95,6	16	7,5	16,7
DM380	*F. prisca*	94,1	17,2	6,8	16,8

an age older than 51000 yr BP for the base of the LTTF while the top is exposed as the present-day ground surface (Varela, 1976; Heusser, 1983; Núñez et al., 1994; Valero-Garcés et al., 2005). The LTTF consists of eight members according to different sedimentary attributes (Varela, 1976) (Fig. 1D). The specimens reported in this work were collected at the unconformity between member 5 and member 6, at around 1.9–2.4 m depth, where two archaeological occupation spatially differentiated have been detected: Taguatagua 1 (TT-1) and Taguatagua 2 (TT-2) (Montané, 1968; Varela, 1976; Núñez et al., 1994). According to several

radiocarbon dates (Montané, 1968; Heusser, 1983; Núñez et al., 1994; Valero-Garcés et al., 2005), this deposition event occurred between ~13590 and 11070 cal yr BP, but anthropic occupations TT-1 and TT-2 were dated around 12600 and 11600 cal yr AP respectively (Núñez et al., 1994; Labarca et al., 2020). In summary, the rallid bones studied here come from the late Pleistocene – early Holocene transition which, according to paleoenvironmental and paleoclimate reconstructions, corresponds to a phase of abrupt changes from wet/cold to arid/dry conditions in central Chile (Heusser, 1990; Kaiser et al., 2005; Valero-Garcés et al., 2005).

Rallid bones were stratigraphically associated with several other bird taxa, such as *Anas* cf. *A. flavirostris*, *Anas* cf. *A. georgica*, *Lophonetta* cf. *L. specularioides*, *Podiceps major*, *Zenaida* sp., *Geranoaetus melanoleucus* and *Milvago chimango*, but also with numerous mammalian taxa from a diverse sort of families such as Gomphotheriidae, Equidae, Cervidae, Canidae, Didelphidae, Octodontidae, Abrocomidae, Echimyidae and Cricetidae, as well as with fish (*Odonthestes* sp.), anurans

(*Calyptocephalella gayi* and *Rhinella* sp.), reptiles (cf. *Philodryas* sp.) and mollusks (*Biomphalaria taguataguensis*) (Alarcón, 2016; Labarca et al., 2020).

4. Systematic paleontology

Class Aves Linnaeus (1758)
Order Gruiformes Bonaparte (1854)
Superfamily Ralloidea Vigors (1825)
Family Rallidae Rafinesque (1815)
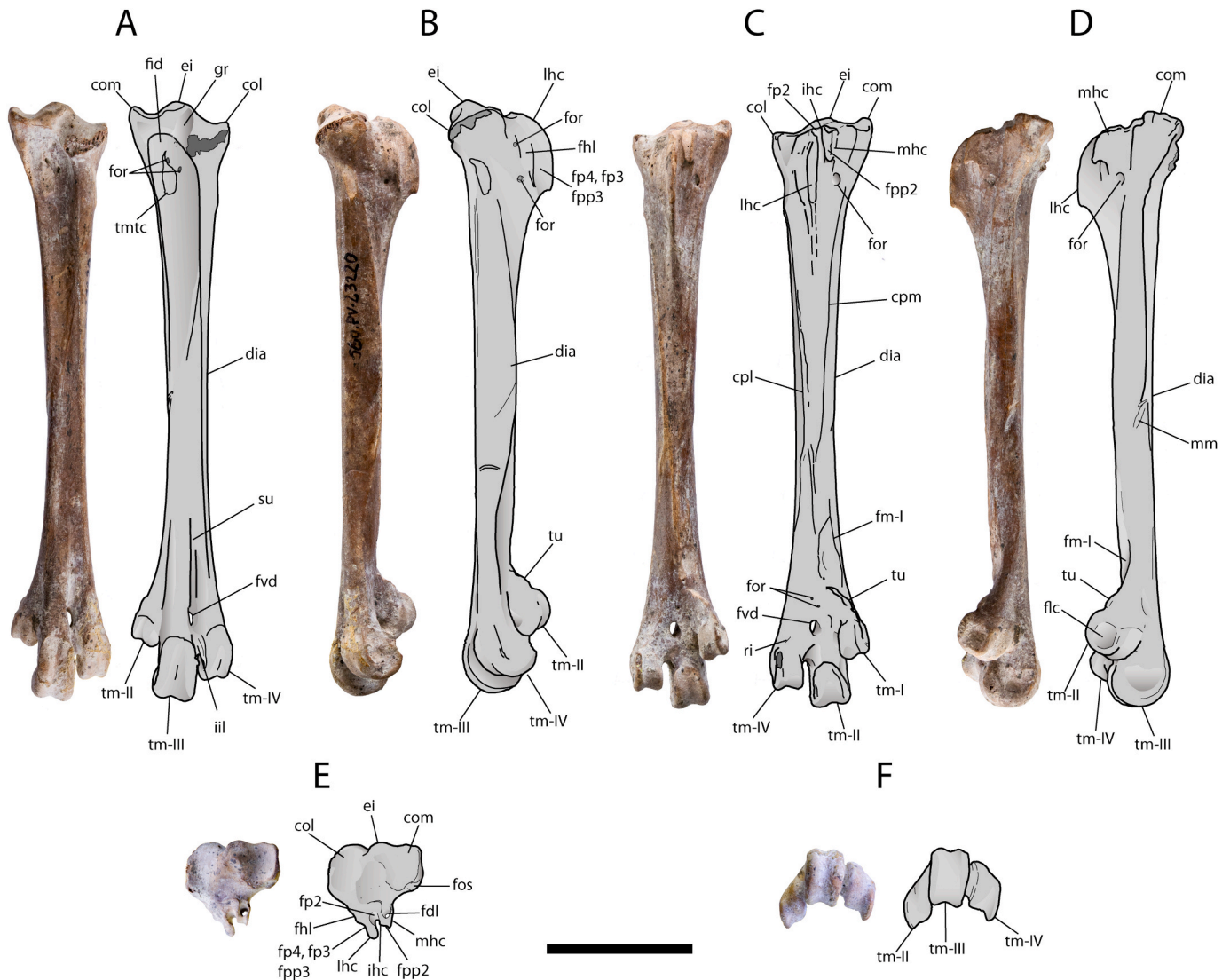Genus *Fulica* Linnaeus (1758)
Type species *Fulica atra* Linnaeus (1758)
Fulica montanei sp. nov. (Figs. 2 and 3; Table 1).
**Holotype:** SGO.PV.23220, a complete left tarsometatarsus.
Paratype: SGO.PV.23221, a left tarsometatarsus without the *cotyla medialis* and fragmented *trochlea metatarsi II*.
Referred material: SGO.PV.23240, a distal portion of a left

Fig. 2. *Fulica montanei* sp. nov. (SGO.PV.23320, holotype). Left tarsometatarsus in dorsal (**A**), lateral (**B**), plantar (**C**), medial (**D**), proximal (**E**) and distal (**F**) views. Scale bar: 20 mm. Abbreviations: col: *cotyla lateralis*; com: *cotyla medialis*; cpm: *crista plantares medialis*; cpl: *crista plantares lateralis*; dia: diaphysis; ei: *eminentia intercotylaris;* fdl: canal for tendon of *musculus flexor digitorum longus;* fhl: sulcus for tendon of *musculus flexor hallucis longus*; flc: *fovea ligamenti collateralis*; fp2: sulcus for tendon of *musculus flexor perforatus digiti 2;* fpp2: sulcus for tendon of *musculus flexor perforans et perforatus digiti 2;* fp4, fp3, fpp3: sulcus for tendons of *musculus flexor perforatus digiti IV, m. flexor perforatus digiti III, and m. flexor perforans et perforatus digiti III;* fm-I: *fossa metatarsi I*; for: foramina; fos: fossa; fvd: *foramen vasculare distale*; fid: *fossa infracotylaris dorsalis;* gr: groove; ihc: intermediate hypotarsal crest; iil: *incisura intertrochlearis lateralis;* lhc: lateral hypotarsal crest; mhc: medial hypotarsal crest; mm: muscular mark; su: sulcus; ri: ridge; tm-II: *trochlea metatarsi II*; tm-III: *trochlea metatarsi III*; tm-IV: *trochlea metatarsi IV*; tmtc: *tuberositas musculi tibialis cranialis;* tu: tubercle.
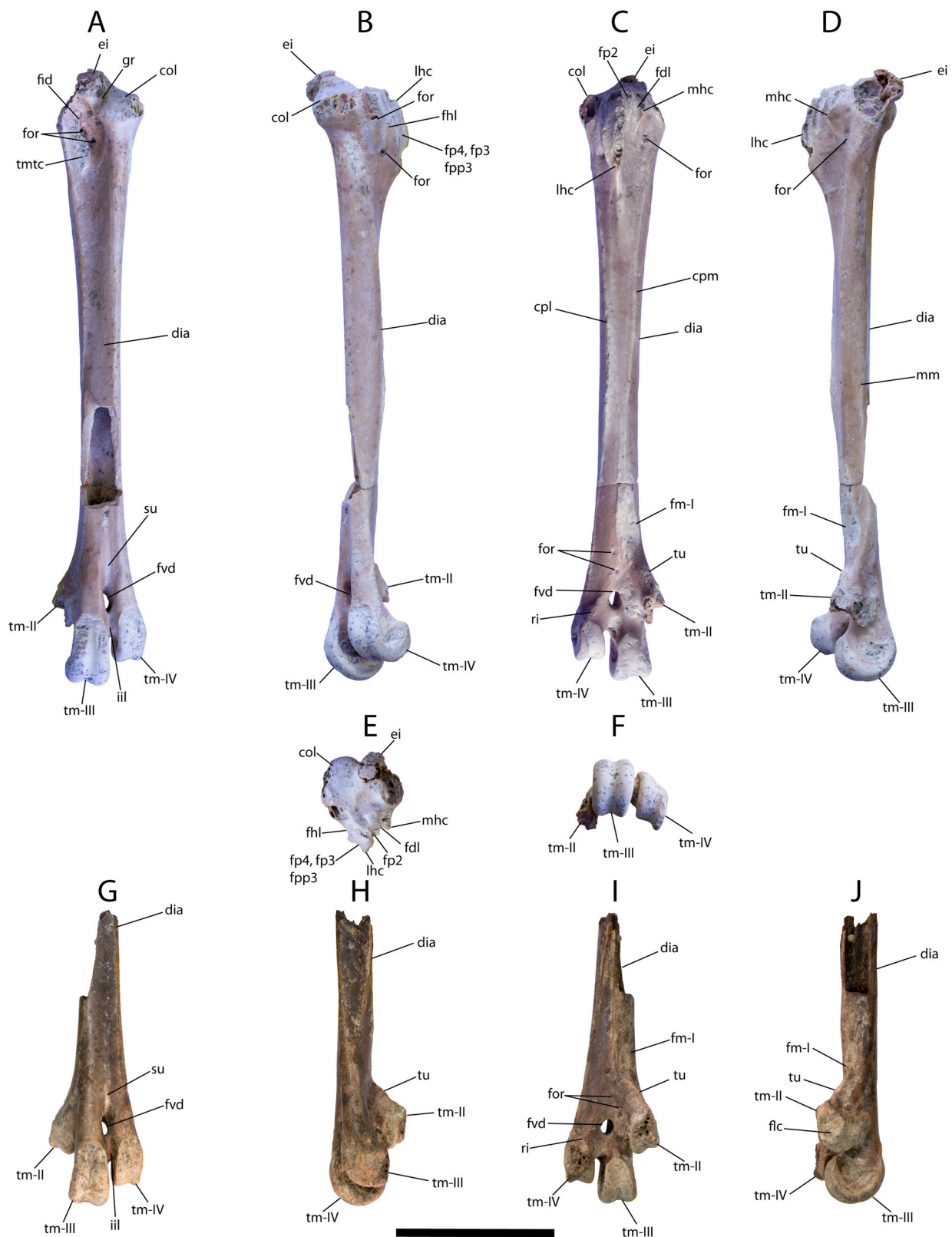
Fig. 3. Paratype and referred material of *Fulica montanei* sp. nov. **A-F,** left tarsometatarsus (paratype, SGO.PV.23321) in dorsal (**A**), lateral (**B**), plantar (**C**), medial (**D**), proximal (**E**), and distal (**F**) views. **G-J,** distal portion of a left tarsometatarsus (referred material, SGO.PV.23240) in dorsal (**G**), lateral (**H**), plantar (**I**), and medial (**J**) views. Scale bar; 20 mm. Abbreviations: col: *cotyla lateralis*; com: *cotyla medialis*; cpm: *crista plantares medialis*; cpl: *crista plantares lateralis*; dia: diaphysis; ei: *eminentia intercotylaris*; fdl: canal for tendon of *musculus flexor digitorum longus;* fhl: sulcus for tendon of *musculus flexor hallucis longus*; fp2: sulcus for tendon of *musculus flexor perforatus digiti 2;* fp4, fp3, fpp3: sulcus for tendons of *musculus flexor perforatus digiti IV, m. flexor perforatus digiti III, and m. flexor perforans et perforatus digiti III;* fm-I: *fossa metatarsi I*; for: foramina; fvd: *foramen vasculare distale*; flc: *fovea ligamenti collateralis*; fid: *fossa infracotylaris dorsalis*; gr: groove; lhc: lateral hypotarsal crest; mhc: medial hypotarsal crest; iil: *incisura intertrochlearis lateralis*; mm: muscular mark; su: sulcus; ri: ridge; tm-II: *trochlea metatarsi II*; tm-III: *trochlea metatarsi III*; tm-IV: *trochlea metatarsi IV;* tmtc: *tuberositas musculi tibialis cranialis*; tu: tubercle.

tarsometatarsus.

Etymology: In honor of Julio Montané, the archaeologist who started the scientific research at Laguna de Tagua Tagua with the excavation of the archaeo-paleontological site TT-1.

Locality and Horizon: TT-1 (SGO.PV.23220, SGO.PV.23221) and TT-2 (SGO.PV.23240) archaeo-paleontological sites, Laguna de Tagua Tagua, late Pleistocene - early Holocene, O'Higgins region, Central Chile.

Diagnosis: *Fulica montanei* is diagnosed based on the following combination of traits: Large and robust tarsometatarsus within the size range of *Fulica cornuta*, but above the size range of other American members of *Fulica*, such as *Fulica armillata, Fulica rufifrons, Fulica leucoptera, Fulica ardesiaca* and *Fulica americana*; *fossa infracotylaris dorsalis* mediolaterally wide and deeply excavated; *trochlea metatarsi III* medioloaterally wide in dorsal view, with its medial and lateral edge not converging proximally; tubercle situated in the proximal edge of the *trochlea metatarsi II* plantarly displaced with respect to the distal ridge of the *fossa metatarsi I*; ridge diagonally extended on the plantar surface of the *trochlea metatarsi IV* poorly developed.

Description and comparisons: The specimens SGO.PV.23220, SGO.PV.23221 and SGO.PV.23240 are nearly identical morphologically, nevertheless, SGO.PV.23221 is slightly smaller than SGO.PV.23220 and lacks the *cotyla medialis* and part of the *trochlea metatarsi II* (Figs. 2 and 3). The specimen SGO.PV.23240 corresponds to a distal portion of a left tarsometatarsus (Fig. 3).

In proximal view, the lateroplantar edge of the *cotyla medialis* in SGO.PV.23220 has a proportionally small fossa with respect to the articular surface of the *cotyla medialis* (Fig. 2E). This character in *F. cornuta* is much more developed and broader mediolaterally. In the specimen SGO.PV.23221 the *cotyla medialis* is not preserved (Fig. 3E).

For both SGO.PV.23220 and SGO.PV.23221, in dorsal view (Figs. 2 and 3), the surface of the diaphysis is flat and transversely compressed, as in *Fulica* (Wetmore, 1924; Olson, 1973; Livezey, 1998; Boles, 2005). The lateral edge is more prominent than the medial one, a feature that is especially marked in the proximal half of the diaphysis, in which the medial edge is less developed cranially than the lateral one. These traits are also observed in *F. armillata, F. rufifrons, F. ardesiaca, F. leucoptera* and *F. gigantea*. In *F. montanei* the proximal third of the medial ridge in dorsal view is robust, while in *F. gigantea* it is a relatively narrow ridge that continues to the cranial edge of the *cotyla lateralis*.

The *fossa infracotylaris dorsalis* is proportionally more excavated and wider than in *F. armillata, F. gigantea, F. rufifrons, F. ardesiaca* and *F. leucoptera*. In this fossa the *tuberositas musculi tibialis cranialis* is large and distinctive, with a flat dorsal surface as in the genus *Fulica* (Wetmore, 1924; Olson, 1973; Livezey, 1998; Boles, 2005). This fossa is approximately twice as long as wide and is medially located. This tuberosity is flanked by two small foramina; one located on its proximal edge, and the other on its proximolateral edge, almost at the middle of the *fossa infracotylaris dorsalis*. Unlike in *F. gigantea*, in *F. montanei* these foramina are proportionately small. In *F. cornuta* the *tuberositas musculi tibialis cranialis* is proportionately more robust than in *F. montanei*. The *cotyla lateralis* is more projected proximally than the *cotyla medialis*, as in *F. armillata, F. rufifrons, F. leucoptera, F. ardesiaca, F. gigantea* and *F. americana*.

In the specimen SGO.PV.23220, the *eminentia intercotylaris* is robust, nearly rounded and slightly more developed proximally than the *cotyla medialis*. This structure is partially preserved in SGO.PV.23221. The proximal surface of the *eminentia intercotylaris* in *F. montanei* is rounded, while in *F. gigantea* and *F. cornuta* it is flat. Between the *eminentia intercotylaris* and the *cotyla lateralis* there is a well-marked groove that begins at the proximal edge of the *fossa infracotylaris dorsalis* and extends over the craniolateral surface of the *eminentia intercotylaris*, as in the reference specimens of *Fulica*.

The lateral hypotarsal crest is prominent and extended proximodistally, as in other members of Rallidae (Boles, 2005). The lateral hypotarsal crest is approximately three times longer than the medial

hypotarsal crest like in other tarsometatarsi of extant species of *Fulica* used as references. The medial hypotarsal crest, or *crista medialis flexoris digitorum longus*, as is defined in Mayr (2015), is reduced to a proximodistally very short osseous sheet, which is a feature considered as an autapomorphy of Ralloidea (Mayr, 2004, 2015). The medial hypotarsal crest is partially preserved in SGO.PV.23221. In *F. montanei* the lateral hypotarsal crest is more plantarly projected with respect to the medial and intermediate hypotarsal crests than in *F. gigantea* and *F. rufifrons*. The plantar edge of the lateral hypotarsal crest is thin along its entire length, while in *F. cornuta* it is more robust. In medial view, the distal end of the lateral hypotarsal crest ends at a tip, and then decreases towards the distal end, while in *F. gigantea* the distal end of the lateral hypotarsal crest is more rounded. Laterally to the lateral hypotarsal crest, there is a parallel longitudinal ridge, which is much less developed than in *F. cornuta*. Dorsally to this ridge, there is a second less marked and dorsoventrally shorter ridge. This second ridge is much more prominent in *Fulica cornuta* than in *Fulica montanei*. The most plantarly located ridge marks the limit that separates the sulci through which flexor tendons pass. The sulcus limited by the plantar border of the lateral hypotarsal crest and the lateral ridge of the most plantar position represents the area through which the tendons of *musculus flexor perforatus digiti IV* (fp4), *musculus flexor perforatus digiti III* (fp3), and *musculus flexor perforans and perforatus digiti III* (fpp3) pass (Mayr, 2004, 2015, 2019). The lateral plantar and dorsal ridges limit a groove more dorsally located through which the tendon of the *musculus flexor hallucis longus* (fhl) pass. This sulcus is dorsoplantarly narrower than the sulcus for the tendons of the fp4, fp3 and fpp3 muscles. Located laterally to the medial hypotarsal crest there is a foramen, which is proportionally larger than the one present in the reference specimen of *F. gigantea*. Additionally, there is a second foramen on the lateral surface of the proximal tarsometatarsal region, which is located more proximally (Fig. 2B). As in several members of Rallidae, in proximal view, the hypotarsus is broadly triangular and a sulcus and a canal are present (Boles, 2005; Mather et al., 2018). A bony canal for the tendon of the *musculus flexor digitorum longus* (fdl) is present (Mayr, 2004; 2015, 2019), which is formed by the medial al intermediate hypotarsal crests. This canal is partially preserved in the specimen SGO.PV.23221 since both the medial and intermediate hypotarsal crest are broken. Lateral to this osseous canal are sulci for the tendon of the *musculus flexor perforatus digiti 2* (fp2), and for the tendon of the *musculus flexor perforans et perforatus digiti 2* (fpp2) as represented by Mayr (2004, 2015, 2019). These sulci are between the lateral and intermediate hypotarsal crests as in the reference specimens of *F. cornuta* and *F. leucoptera*. In contrast, in *F. gigantea*, the sulci for the tendons of fp2 and fpp2 are plantarly closed by the lateral and intermediate hypotarsal crests. In *F. rufifrons* and *F. armillata* this condition is variable, since some specimens were observed with open sulci for the tendons of the fp2 and fpp2 muscles, while in other specimens these sulci are plantarly closed. In the specimen SGO.PV.23221 the sulcus for the tendon of fpp2 is not preserved, because the medial and intermediate hypotarsal crests are broken (Fig. 3E).

The diaphysis is transversely compressed proximal to the distal trochlea, as in the genus *Fulica* (Wetmore, 1924; Olson, 1973; Livezey, 1998; Boles, 2005) and is proportionally more robust than *F. armillata*. In medial and lateral view, the plantar profile of the diaphysis of the tarsometatarsi of *F. montanei* is slightly convex, while in *F. gigantea* is straight. In the medial surface of the diaphysis, a diagonally arranged muscular mark is observed, as in other species of *Fulica*. In a lateral view and at the proximal end, a small foramen is found located on the laterodistal edge of the medial hypotarsal crest. This foramen is also present in *F. gigantea*, although it is proportionately larger.

In the distal portion, a narrow longitudinal groove is observed, which deepens distally and continues with the oval *foramen vasculare distale*, whose longitudinal axis is slightly longer than its transverse axis. Just below the *foramen vasculare distale* there is a marked groove that extends to the proximal edge of the *incisura intertrochlearis lateralis*, as in the reference specimens of *Fulica*. The *trochleae metatarsorum* are robust as

in *Fulica cornuta*. Laterally, the *trochlea metatarsi III* of *F. montanei* is mediolaterally wide, its medial and lateral ridges are almost parallel to each other as in *F. cornuta* and *F. gigantea,* and do not converge proximally. In contrast, these ridges in *Fulica armillata* converge proximally in an acute angle. The *trochlea metatarsi II* is proximally positioned, as in other members of *Fulica* (Wetmore, 1924; Olson, 1973; Livezey, 1998; Boles, 2005; Cenizo et al., 2015). The *trochlea metatarsi III* is more distally extended than the *trochlea metatarsi II* and *IV*, and the *trochlea metatarsi IV* is plantarly recessed, as in *F. armillata*, *F. rufifrons*, *F. ardesiaca*, *F. gigantea*, *F. cornuta* and *F. americana*. The greater distal extension of the *trochlea metatarsi III* than the *trochlea metatarsi IV* is a typical character of Rallidae (Boles, 2005). Furthermore, the distal extension of the *trochlea metatarsi IV* and the proximal position of the *trochlea metatarsi II* are diagnostic characteristics of the genus *Fulica* (Wetmore, 1924; Olson, 1973; Livezey, 1998; Boles, 2005; Cenizo et al., 2015). The distal edge of the *trochlea metatarsi IV* does not reach the level of the proximal edge of the *incisura intertrochlearis lateralis*. The *trochlea metatarsi IV* in SGO.PV.23221 is incomplete.

In plantar view, the *cristae plantares medialis* and *lateralis* are observed, which progressively reach each other distally, until they converge approximately at the beginning of the distal third. From this same point another ridge emerges, which opens laterally and extends to the proximal edge of the *fovea ligamenti collateralis* of the *trochlea metatarsi IV*, like other reference specimens of *Fulica*. On the *foramen vasculare distale*, the tarsometatarsus of *F. montanei* exhibits two small foramina which are very close to each other. In *F. gigantea* both foramina are located more proximally, close to the mediodistal edge of the *fossa*

metatarsi I. The *trochlea metatarsi III* in *F. montanei* is mediolaterally narrower than in *F. cornuta*, and the proximal edge of this trochlea forms an acute angle oriented proximally, as in *F. gigantea, F. armillata*, *F. rufifrons* and *F. leucoptera*. In *F. cornuta* the proximal edge of the *trochlea metatarsi III* is wide and horizontal, with rounded lateral and medial edges. Plantarly, the proximal section of *trochlea metatarsi III* is mediolaterally wider than *F. armillata*, as in its dorsal surface. The proximal edge of the *trochlea metatarsi II* has a low tubercle, which is evident in medial view. Unlike in *F. armillata*, this tubercle is plantarly displaced with respect to the distal edge of the *fossa metatarsi I*; resulting in this tubercle being closer to the medioplantar edge of the *trochlea metatarsi II*. In the plantar surface of the *trochlea metatarsi IV* of *F. armillata*, *F. cornuta*, *F. ardesiaca, F, gigantea* y *F. rufifrons* there is a marked flange that approximately emerges at the level of the *foramen vasculare distale*, extending diagonally until the proximal portion of the lateral edge of the *trochlea metatarsi IV*. On the contrary, in the three metatarsi of *F. montanei* this flange is poorly developed.

The scatter plot built with GL and Bp measurements (Fig. 4; Table 1) situates the specimen SGO.PV.23220 among the biggest species of *Fulica*, being comparable with the tarsometatarsus of the extant crested coot (*F. cornuta*) and the smallest specimens of the extinct form *F. prisca* from New Zealand (Fig. 4A). Principal component analysis confirms the above-mentioned, since the first component, which explain 99,76 of the variance, places SGO.PV.23220 together with *F. cornuta*, clearly separated from species of central Chile, *F. armillata*, *F. rufifrons*, *F. leucoptera* and also from the Andean *F. ardesiaca* (Fig. 4B). These results also point out that the biggest extant forms *F. gigantea* and *F. cornuta,* both
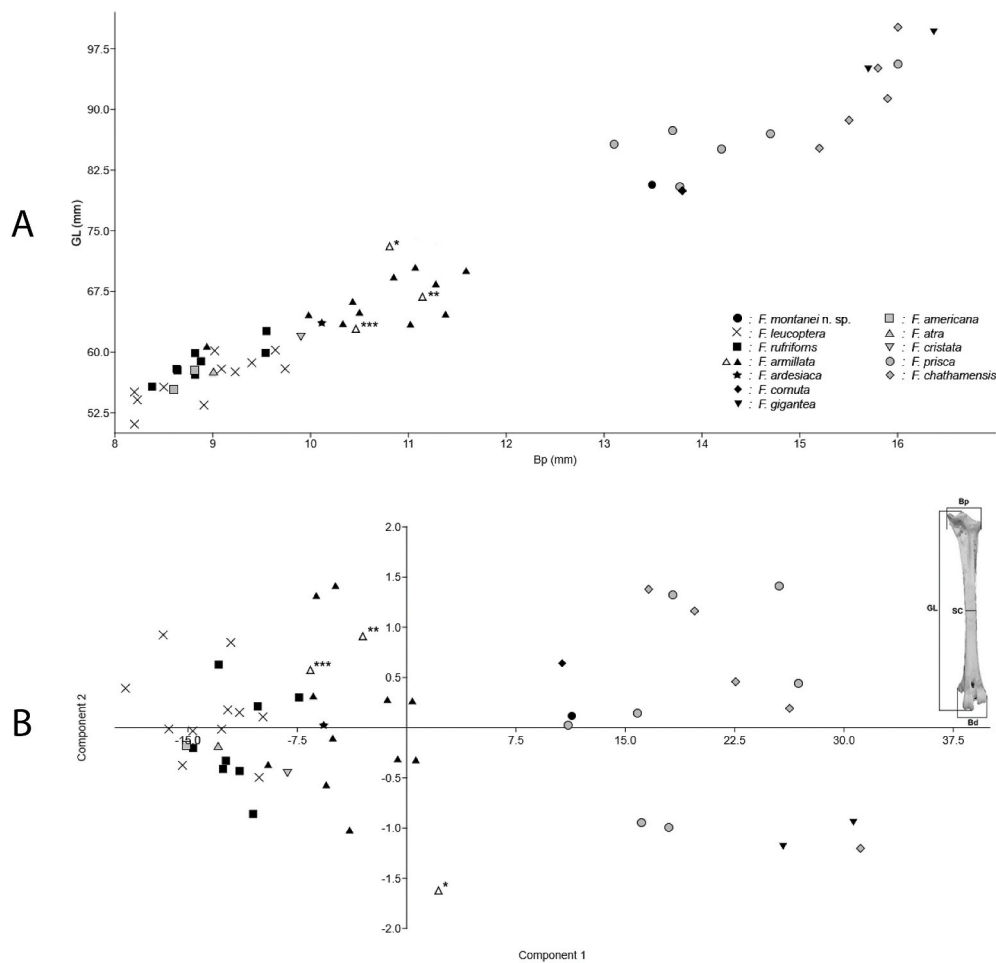

Fig. 4. Bivariate and multivariate analysis. (**A**), Metatarsi bivariate scatter diagram considering GL and Bp. (**B**) Principal component analysis considering metatarsi measurements GL, Bp, SC and Bd. *: SGO.PV. 27789; **: SGO.PV.23334; ***: SGO.PV.23236. Metrical data from Table 1. White triangle corresponds to fossil specimens.

sympatric in the Andean area, can be metrically separated (Livezey, 2003). Interestingly, the small South American extant *Fulica*, that includes *F. armillata*, *F. ardesiaca*, *F. rufifrons* and *F. leucoptera*, are clearly arranged on a gradient of size, which agrees with the reported body mass and body length of these species (Livezey, 2003). Furthermore, it is possible to observe two subsets of species composed by the smallest *F. leucoptera*/*F. rufifrons*, and the proportionally larger *F. ardesiaca*/*F. armillata*. Finally, the size range observed inside *F. leucoptera* and *F. armillata*, which correspond to the taxa with the highest number of reference specimens, could be related to sexual dimorphism (Livezey, 2003).

Fulica armillata Vieillot (1817) (Fig. 5A–K).

Referred material: SGO.PV.27784, left humerus; SGO.PV.27785, right humerus; SGO.PV.27786, incomplete right humerus; SGO.PV.27787; incomplete right humerus; SGO.PV.27788, left coracoid; SGO.PV.23244, right coracoid; SGO.PV.23247, distal half of right tibiotarsus; SGO.PV.27789, left tarsometatarsus; SGO.PV.23236, right tarsometatarsus; SGO.PV.23239, distal half of left tarsometatarsus; SGO.PV.23334, right tarsometatarsus.

Locality and horizon: TT-1 (SGO.PV. 27784, 27785, 27786, 27787, 27788, 27789, 23236, 23334) and TT-2 (SGO.PV. 23239, 23244, 23247) archaeo-paleontological sites, Laguna de Tagua Tagua, late Pleistocene - early Holocene, O'Higgins region, Central Chile.

Description and comparisons: Both SGO.PV.27784 and SGO.PV.27785 are humeri morphologically identical, with the latter in the size range of *F. armillata* (Fig. 5A and B). Both humeri are slightly dorsally curved. The *margo caudalis* is well developed, which confers to the proximal portion of the diaphysis a triangular section. Distally, the diaphysis is tubular. The *fossa pneumotricipitalis* is wide and well-excavated and is caudolaterally oriented. The *incisura capitis* is oval-shape, wide, deeply excavated, and it extends between the proximoventral ridge of the *caput humeri* and the proximal portion of the *margo caudalis*. The *caput humeri* is rounded, and presents a triangular profile in caudal and cranial view. The *tuberculum ventrale* is well-developed caudally, but its articular surface is oriented dorsocaudally. In turn, the *tuberculum dorsale* is less developed than the *tuberculum ventrale* and its articular surface is caudally oriented. In distal view, the *sulcus musculi scapulotricipitalis* is well excavated and extended from the distal surface to the caudal surface. The *fossa olecrani* is dorsoventrally wide and distally continues on the *sulcus musculi humerotricipitis*, which is shallow. The *epicondylus ventralis* is blunt and is ventrally projected. Ventrally both humeri are slightly sigmoidals. Dorsally, the *crista deltopectoralis* is cranially extended and its proximal and cranial ridges constitute an obtuse angle. The latter is slightly concave and almost parallel to the diaphysis. Distally, the cranial ridge of the *crista deltopectoralis* conforms another obtuse angle with its distal ridge, although this angle is less cranially extended than the proximal angle. In the cranial surface, the *sulcus ligamentus transversus* is restricted to the proximoventral edge of the proximal portion, below the ventral border of the *caput humeri*. The latter is narrow ventrally and wide dorsally, and its deepest point is located in the ventral portion. The *impressio musculi coracobrachialis cranialis* is wide and shallow and is dorsally flanked by the *crista deltopectoralis*. Distally, the *fossa musculi brachialis* is also wide and shallow. Its proximal edge forms an acute angle medially inclined. The *tuberculum supracondylare ventrale* has a pyramid-shape and is cranially oriented. The *processus supracondylaris dorsalis* is less developed than the *tuberculum supracondylare ventrale* and is dorsocranially oriented. Cranially, the *condylus dorsalis* has an oval-shape and its proximal portion is proximomedially curved. The *condylus ventralis* has also an oval-shape and its longest axis is dorsoventrally oriented. In the specimen SGO.PV.27785 both condyles are slightly stouter than SGO.PV.27784, a feature probably related to intraspecific variation. In both humeri, the *processus flexorius* is poorly distally projected.

The specimens SGO.PV.27786 and SGO.PV.27787 correspond to two incomplete right humeri (Fig. 5C and D). In spite of that, both elements lack the *caput humeri*, the size and proportions of the distal epiphysis

agree with those observed in SGO.PV.27785 and SGO.PV.27784 and also with the reference material of *F. armillata*.

The specimen SGO.PV.23247 corresponds to a distal portion of a right tibiotarsus (Fig. 5E). Its size and proportions are in the range of *F. armillata*. The *sulcus extensorius* deepens distally, until it generates the *canalis extensorius*. The *pons supratendineus* is proximodistally wide. Unlike in *F. ardesiaca*, the lateral half of the dorsal ridge of the *pons supratendineus* is proximally higher, as in *F. armillata* and *F. rufifrons*. Unlike in *F. rufifrons*, SGO.PV.23247 is mediolaterally wide. The distal opening of the *canalis extensorius* is wide. The *incisura intercondylaris* is mediolaterally wide as in the reference specimens of *Fulica*. The *condylus lateralis* is much stouter than the *condylus medialis*. In cranial view, the medial surface of the cranial area of the *condylus medialis* presents a crest that emerges from its proximal ridge and extends distally. This crest is stouter than in *F. rufifrons*. In caudal view, the *trochlea cartilaginis tibialis* is mediolaterally wide and its lateral and medial ridges are nearly parallel to each other, although the proximal ridge of the medial ridge is slightly curved medially.

The four tarsometatarsi SGO.PV.27789, SGO.PV.23239, SGO.PV.23334 and SGO.PV.23236 are morphologically similar (Fig. 5F–I). The specimen SGO.PV.27789 is a left tarsometatarsus without the hypotarsal crests (Fig. 5F). The specimen SGO.PV.23239 corresponds to a distal half of a left tarsometatarsus (Fig. 5G). Finally, the specimens SGO.PV.23334 and SGO.PV.23236 correspond to a two complete right tarsometatarsi (Fig. 5H and I). In the four specimens the dorsal surface is flat as in Rallidae (Boles, 2005). In the complete bones, the proximal portion is slightly medially rotated as in other reference specimens of *Fulica*. Due to this, in the diaphysis, the proximal half of the dorsolateral edge is more prominent than the dorsomedial one. In proximal view, the specimens SGO.PV.23334 and SGO.PV.23236 are nearly triangular in shape, but with the medial and lateral edges of the cotyles arranged parallel to each other. An osseous canal for the tendon of the *musculus flexor digitorum longus*, and sulci for the tendons of *the musculus flexor perforatus digiti II* (fp2) and for the *musculus flexor perforans and perforatus digiti II* (fpp2) are present, as in other members of Rallidae (Mayr, 2004, 2015, 2019; Boles, 2005; Mather et al., 2018). As in Rallidae, the lateral hypotarsal crest is more plantarly and distally extended than the other hypotarsal crests (Boles, 2005), which are partially eroded. The *cotyla medialis* is higher than *cotyla lateralis*. The articular surface of the *cotyla medialis* is concave and proximally has an oval-shape with its longest axis dorsoventrally oriented. In turn, the articular surface of the *cotyla lateralis* is convex, extends dorsally and lacks dorsal ridge as in *cotyla medialis*. The *eminentia intercondylaris* is rounded dorsally and proximally flattened. There is a short sulcus below this structure, which extends proximolaterally and separated from *cotyla lateralis*. The *fossa infracotylaris dorsalis* is well excavated. In this fossa the *tuberositas musculi tibialis cranialis* is located close to its medial ridge. The *tuberositas musculi tibialis cranialis* is elongated proximodistally and distinctive, as in other members of *Fulica* (Wetmore, 1924; Olson, 1973; Livezey, 1998; Boles, 2005), and is mediolaterally narrow. In the tarsometatarsi, the diaphysis is slender and narrow mediolaterally in anterior and posterior view. Distally, there is a longitudinal sulcus which in its distal end connects with the *foramen vasculare distale*, which is small and rounded. In the specimens studied, as in other rallids, the *trochlea metatarsi IV* is shorter than the *trochlea metatarsi III*, and the *trochlea metatarsi II* is much shorter than the *trochlea metatarsi IV*, which also is plantarly retracted (Boles, 2005) and exhibits a mild medial rotation. The three trochleae possess sulcus that runs the entire articular surface. Plantarly, the *cristae plantares medialis* and *lateralis* are located. The *crista plantaris medialis* bifurcates near to the beginning of the distal end of the bone; one of these crests connects to the medial ridge of the *fossa metatarsi I*, while the other continues until the lateral surface of the *trochlea metatarsi IV*.

According to bivariate and multivariate analysis, the tarsometatarsi SGO.PV.23334 and SGO.PV.23236 are in the range of the reference specimens of *F. armillata*. SGO.PV.27788 is slightly longer than *F. armillata* but is clearly smaller than the largest coots such as *F. cornuta*
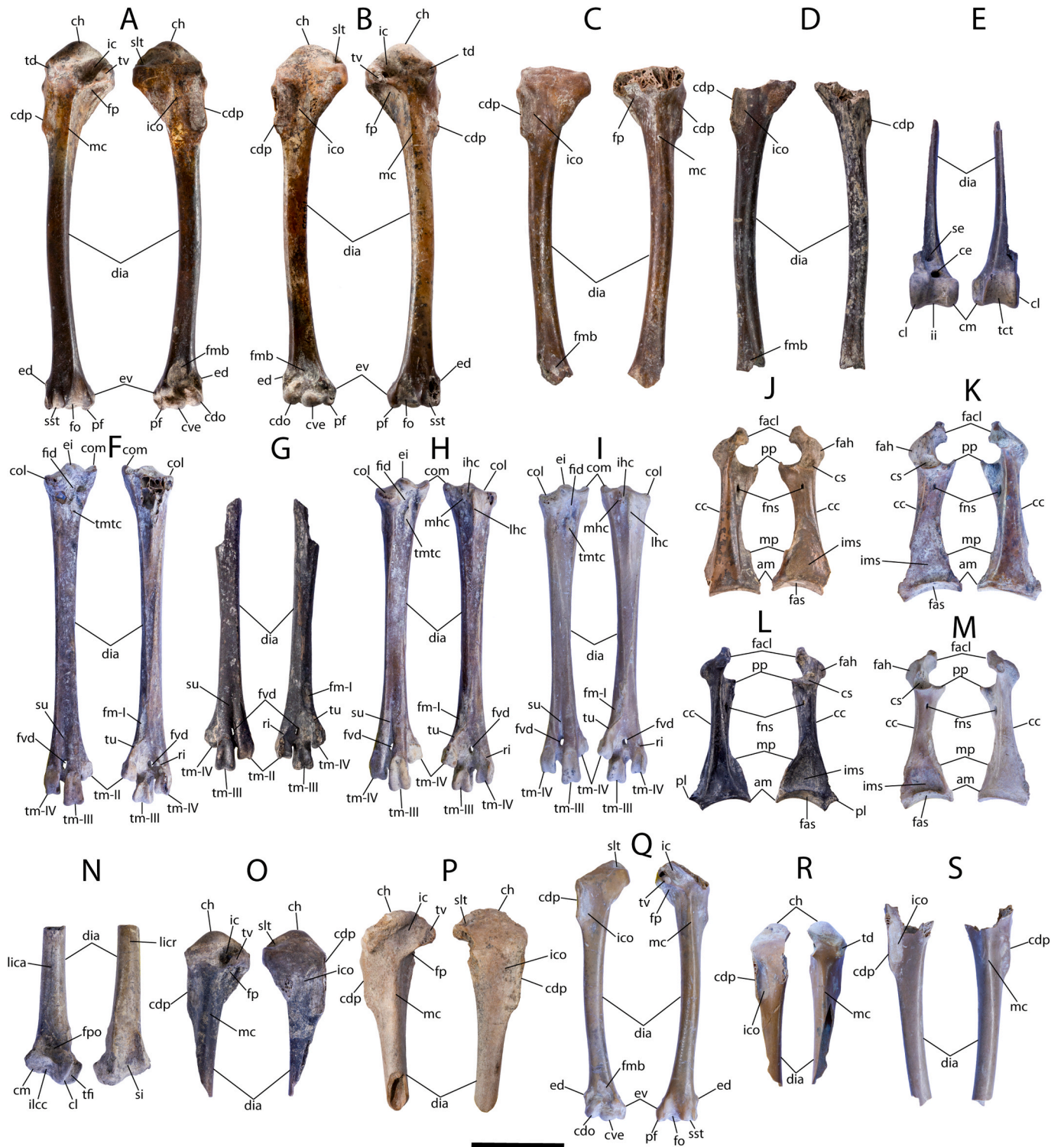
(caption on next page)

Fig. 5. Extant fossil rallid bones. (**A**), *Fulica armillata*, left humerus (SGO.PV.27784) in caudal (left) and cranial (right) views. (**B**) *Fulica armillata*, right humerus (SGO.PV.27785) in cranial (left) and caudal (right) views. (**C**) *Fulica armillata*, incomplete right humerus (SGO.PV.27786) in cranial (left) and caudal (right) views. (**D**) *Fulica armillata*, incomplete right humerus (SGO.PV.27787) in cranial (left) and caudal (right) views. (**E**) *Fulica armillata*, distal half of right tibiotarsus (SGO.PV.23247) in cranial (left) and caudal (right) views. (**F**) *Fulica armillata*, right tarsometatarsus (SGO.PV.27789), in dorsal (left) and plantar (right) views. (**G**) *Fulica armillata*, distal half of left tarsometatarsus (SGO.PV.23239), in dorsal (left) and plantar (views). (**H**) *Fulica armillata*, right tarsometatarsus (SGO.PV.23334), in dorsal (left) and plantar (right) views. (**I**) *Fulica armillata*, right tarsometatarsus (SGO.PV.23236) in dorsal (left) and plantar (right) views. (**J**) *Fulica armillata*, right coracoid (SGO.PV.23244), in ventral (left) and dorsal (right) views. (**K**) *Fulica armillata*, left coracoid (SGO.PV.27788), in dorsal (left) and ventral (right) views. (**L**) *Fulica rufifrons*, right coracoid (SGO.PV.23241), in ventral (left) and dorsal (right) views. (**M**) *Fulica cf. F. rufifrons*, left coracoid (SGO.PV.23245), in dorsal (left) and ventral (right) views. (**N**) *Fulica cf. ardesiaca*, distal portion of right femur (SGO.PV.23224) in caudal (left) and cranial (views). (**O**) *Fulica cf. ardesiaca*, proximal portion of left humerus (SGO.PV.23234) in cranial (left) and caudal (right) views. (**P**) *Fulica sp.*, proximal portion of left humerus (SGO.PV.23223) in caudal (left) and cranial (right) views. (**Q**) *Pardirallus sanguinolentus*, right humerus (SGO.PV.23283) in cranial (left) and caudal (right) views. (**R**) Rallidae indet., proximal portion of a right humerus (SGO.PV.23284) in cranial (left) and (caudal) views. (**S**) Rallidae indet., proximal half of right humerus (SGO.PV.23286) in cranial (left) and caudal (right) views. Scale bar: 20 mm. Abbreviations: am: *angulus medialis*; cc: *corpus coracoidei,* cdp: *crista deltopectoralis*; cdo: *condylus dorsalis*; ce: *canalis extensorius*; ch: *caput humeri*; col: *cotyla lateralis*; com: *cotyla medialis*; cve: *condylus ventralis*; cl: *condylus lateralis*; cm: *condylus medialis*; cs: *cotyla scapularis*; dia: *diaphysis*; ed: *epicondylus dorsalis*; ei: *eminentia intercotylaris*; ev: *epicondylus ventralis*; fah: *facies articularis humeralis*; facl: *facies articularis clavicularis*; fas: *facies articularis sternalis*; fid: *fossa infracotylaris dorsalis*; fns: *foramen nervi supracoracoidei*; fo: *fossa olecrani*; for: *foramina*; fp: *fossa pneumotricipitalis*; fpo: *fossa poplitea*; fm-I: *fossa metatarsi I*: fmb: *fossa m. brachialis*; fvd: *foramen vasculare distale*; lhc: lateral hypotarsal crest; lica: *linea intermus caudalis*; licr: *linea intermus cranialis*; ic: *incisura capitis*; ico: *impressio coracobrachialis*; ihc: intermediate hypotarsal crest; ilcc: *impressio lig. cruciati cranialis*; ims: *impressio m. sternocoracoidei*; ii: *incisura intercondylaris*; mc: *margo caudalis,* mhc: medial hypotarsal crest; mm: muscular mark; mp: medial protrusion of the *extremitas sternalis* of the coracoid; pf: *processus flexorius*; pl: *processus lateralis*; pp: *processus procoracoideus*; ri: ridge; se: *sulcus extensorius*; slt: *sulcus lig. transversus*; sst: *sulcus scap. tricep.*; su: *sulcus*; tct: *trochlea cartilaginis tibialis*; td: *tuberculum dorsale*; tfi: *trochlea fibularis*; tu: tubercle; tv: *tuberculum ventrale*; tm-II: *trochlea metatarsi II*; tm-III: *trochlea metatarsi III*; tm-IV: *trochlea metatarsi IV*; tmtc: *tuberositas musculi tibialis cranialis*.

and *F. gigantea* (Fig. 4A and B).

Right and left coracoids (SGO.PV.23244 and SGO.PV.27788 respectively) are morphologically identical to each other (Fig. 5J and K), and in turn, both are almost indistinguishable from reference specimens of *F. armillata*. Both coracoids are more robust than those of *Fulica rufifrons*, *Fulica leucoptera* and *Fulica ardesiaca*, but their robustness is similar to that of *Fulica armillata*. In dorsal view, the *cotyla scapularis* is wide, well-excavated, with a contour roughly triangular and is dorsally oriented, as in reference specimens of *Fulica, Porphyriops* and *Pardirallus*, and as in other genera of Ralloidea, such as *Porphyrio, Rallina, Canirallus* and *Heliornis* (see Fig. 3 in Mayr and Bochensky, 2016). The *procesus procoracoideus* is well projected medially and is cranioventrally curved as in *Fulica* and as in other genera of Ralloidea, such as *Porphyrio, Pardirallus* and *Gallinula* (see Fig. 3 in Mayr and Bochensky, 2016). The *facies articularis humeralis* is somewhat laterally expanded and presents a triangular contour. The *processus acrocoracoideus* is inclined medially and the *impressio ligamentus acrocorahumeralis* is laterocranially oriented. In both coracoids, the mid-section is dorsally flat and ventrally convex. The *foramen nervi supracoracoidei* is small and is present in the cranial portion of the *corpus coracoidei*, below the *cotyla scapularis*. Distally, the *impressio musculi sternocoracoidei* is concave and is flanked caudally by the cranial rim of the *facies articularis sternalis*. The latter is caudodorsally oriented. In the medial margin of the *extremitas esternalis* there is a medial protrusion, which is a trait present in several taxa of Rallidae, such as *Fulica, Pardirallus* and *Gallinula*, but not in *Sarothrura* and *Canirallus* (Mayr and Bochenski, 2016) The *angulus medialis* is caudally oriented, as in reference specimens of *Fulica,* as well as in *Pardirallus* and *Porphyrio*, but less pronounced than in *Gallinula* (see Fig. 3 in Mayr and Bochensky, 2016). Medially, the longest axis of the *facies articularis clavicularis* is diagonally inclined with respect to the coracoid main axis. The ventral end of the *facies articularis clavicularis* is more cranially located than the dorsal one. The *sulcus musculi supracoracoidei* is wide and diagonally oriented with respect to the longitudinal axis of the coracoid. In ventral view, the sulcus conformed by the curvature of the *processus procoracoideus* is wide and confines the *foramen nervi supracoracoidei*, which is located at the base of the *processus procoracoideus*.

Fulica rufifrons Philippi and Landbeck (1861) (Fig. 5L).

Referred material: SGO.PV.23241, right coracoid.

Locality and horizon: TT-2 archaeo-paleontological site, Laguna de Tagua Tagua, late Pleistocene - early Holocene, O'Higgins region, Central Chile.

Description and comparisons: The size and proportions of SGO.PV.23241 are similar to those observed in *F. rufifrons* and, smaller and more slender than in reference specimens of *F. armillata* (Fig. 5L). The *extremitas omalis* is proportionally smaller than in *Fulica armillata* and *Fulica leucoptera*, as in the coracoid of the Pleistocene of Argentina assigned to *Fulica rufifrons* by Cenizo et al. (2015). The specimen SGO.PV.23241 has a narrower *corpus coracoidei* than *F. armillata*, which agrees with the observations by Cenizo et al. (2015). In dorsal view, the *cotyla scapularis* is well excavated, although to a lesser extent than in *F. armillata*, which agrees with what was observed by Cenizo et al. (2015). The contour of the *cotyla scapularis* is convex laterally and concave dorsomedially. The *facies articularis humeralis* protruding laterally. As in *F. rufifrons*, the *facies articularis humeralis* is slightly concave in its caudal portion and does not reach the caudal edge of the *cotyla scapularis*. By contrast, in *F. armillata* the caudal edge of the *facies articularis humeralis* is convex and reaches the caudal edge of *cotyla scapularis*. The *impressio ligamenti acrocoracohumeralis* is laterocranially oriented with an area proportionally smaller than in *F. armillata*. The *corpus coracoidei* is dorsally flat and ventrally convex. In dorsal view, the *foramen nervi supracoracoidei* is in the cranial portion of the *corpus coracoidei*. The *foramen nervi supracoracoidei* is small and rounded. In the medial margin of the *extremitas esternalis* there is a marked medial protrusion. This trait is present in several taxa of Rallidae, but not in *Sarothrura* and *Canirallus* (Mayr and Bochenski, 2016). Caudally, the *impressio musculi sternocoracoidei* is more concave than in *F. armillata*. In the caudal end, the *impressio musculi sternocoracoidei* is flanked by the cranial ridge of the *facies articularis sternalis*. The articular surface of the *facies articularis sternalis* is dorsocaudally oriented. Its craniocaudal width is greater in this lateral section than in the medial one, as in *F. rufifrons*. By contrast, in *F. armillata,* the craniocaudal width of the *facies articularis sternalis* is almost constant in its entire mediolateral extension. The *angulus medialis* is caudally oriented and is not projected medially, as in *F. rufifrons*. In *F. armillata,* the *angulus medialis* is projected medially. The *processus lateralis* is cuadrangular in shape and its preserved caudal portion is less extended than the cranial one. The cranial portion of the *processus lateralis* is broken, so it is impossible to determine the exact morphology (i.e. if it ended in a dorsally curved process, as in *F. rufifrons*). In medial view, the *sulcus musculi supracoracoidei* of the specimen SGO.PV.23241 and also in reference specimens of *F. rufifrons* is dorsoventrally shorter than in *F. armillata*. The *facies articularis clavicularis* is dorsoventrally less developed than *F. armillata*. In the specimen SGO.PV.23241, the *processus procoracoideus* is incomplete, although the remnant portion is ventrally curved. The *foramen nervi supracoracoidei* is located in a more caudal position with respect to the base of the *processus procoracoideus* than in *F. armillata*. In ventral view, the longitudinal sulcus confined by the *processus*

procoracoideus is cranially narrower than in *F. armillata*. Caudally, the specimen exhibits a medial concavity above the *angulus medialis*, which is slightly less excavated than in *F. armillata*. The medial portion of the caudal end of the SGO.PV.23241 presents a flange craniocaudally narrow, while in *F. armillata* this rim is craniocaudally wide, generating a small flat surface ventrocaudally oriented.

Fulica cf. *F. rufifrons* Philippi and Landbeck (1861) (Fig. 5M).

Referred material. Left complete coracoid (SGO.PV.23245).

Locality and horizon: TT-1 archaeo-paleontological site, Laguna de Tagua Tagua, late Pleistocene - early Holocene, O'Higgins region, Central Chile.

Description and comparisons: The size of the specimen is consistent with that observed in the coracoid of *Fulica rufifrons*, but it is smaller than that of other species of *Fulica* with which it was compared. The *extremitas omalis* is proportionally smaller than in *Fulica armillata*, which is a trait described for the coracoid of *Fulica armillata* by Cenizo et al. (2015). In dorsal view, the *cotyla scapularis* is well excavated, with a laterally convex and medially concave profile, which gives it an approximately triangular profile, as in other species of *Fulica*, as well as in other genera of Ralloidea, such as *Porphyrio*, *Rallina*, *Canirallus* and *Heliornis* (see Fig. 3 in Mayr and Bochensky, 2016). The *facies articularis humeralis* is well projected laterally and its articular surface is dorsolaterally oriented. The *impressio ligamenti acrocoracohumeralis* is poorly excavated and laterally oriented. The dorsal surface of the *corpus coracoidei* is flat, while the ventral surface is convex. The *processus procoracoideus* is well developed medially and cranioventrally curved, and is distinctly set off from the medial edge, as in members of *Fulica* (De Pietri and Mayr, 2014), as well as in other members of Ralloidea, such as *Pardirallus* and *Gallinula* (see Fig. 3 in Mayr and Bochensky, 2016). In the medial margin of the *extremitas esternalis* there is a marked medial protrusion as in several taxa of Rallidae, except by *Sarothrura* and *Canirallus* (Mayr and Bochenski, 2016). The *impressio musculi sternocoracoidei* is well excavated, especially caudally. In the *extremitas sternalis coracoidei*, the *impressio musculi sternocoracoidei* is flanked by the cranial rim of the *facies articularis sternalis*, whose articular surface is dorsocaudally oriented. The *angulus medialis* is caudally curved and very poorly developed medially. The *processus lateralis* is not preserved. The *processus acrocoracoideum* is well projected cranially. In medial view, the *sulcus musculi supracoracoidei* is wide. Below the level of the caudal border of the *processus procoracoideus* the *foramen nervi supracoracoidei* is located, which is craniocaudally elongated and dorsoventrally narrow, such as in reference specimens of *Fulica*, as well as in other members of Ralloidea, such as *Porphyrio* and *Sarothrura* (see Fig. 3 in Mayr and Bochenski, 2016). The *facies articularis clavicularis* is craniocaudally elongated and dorsoventrally narrow. It is inclined, with its dorsal end more anteriorly situated than its ventral one. The ventral end of the *facies articularis clavicularis* is ventrally protruding. In ventral view, a rim is observed in the distal portion of the coracoid, which is slightly more cranially extended in its medial portion.

Fulica cf. *F. ardesiaca* Tschudi (1843) (Fig. 5N-O).

Referred material: A distal portion of right femur (SGO.PV.23224); a proximal portion of left humerus (SGO.PV.23234).

Locality and horizon: TT-1 (SGO.PV.23224) and TT-2 (SGO.PV.23234) archaeo-paleontological sites, Laguna de Tagua Tagua, late Pleistocene - early Holocene, O'Higgins region, Central Chile.

Description and comparisons: The size and proportions of SGO.PV.23224 (Fig. 5N) are almost identical to those observed in *F. ardesiaca*. The diaphysis is tubular and part of the *linea intermus caudalis* is observed on its caudal surface, which extends to the proximal end of the *condylus medialis*. The *crista supracondylaris medialis* is proximally protruding. The *fossa poplitea* is shallow, and inside it has a tenuous transverse crest, which is slightly more developed than in the reference specimens. The *tuberculum musculi gastrocnemialis lateralis* is rounded, flat and its surface is proportionally large. The *condylus lateralis* presents a *crista tibiofibularis* more acute than in *F. armillata* and *F. rufifrons*, but to a similar degree to *F. ardesiaca*. The *crista tibiofibularis* extends more

caudally than the *epicondylus medialis*, and the extension differences in both structures is greater than in *F. armillata*, but similar to *F. rufifrons* and *F. ardesiaca*. The *impressio ligamenti cruciati cranialis* is shallow and ventrocaudally oriented. As in reference specimens of *Fulica*, in SGO.PV.23224 the *sulcus patellaris* is broad and well excavated, with a medial border more dorsally developed, more proximally extended than the lateral one, and medially inclined. The lateral edge is approximately parallel to the longitudinal axis of the element.

In the fragment of humerus SGO.PV.23234 (Fig. 5O, the *caput humeri* has a subtriangular profile in cranial and caudal views, but its proximal profile is rounded, as in other species of *Fulica*. The *incisura capitis* is highly excavated and rounded. The *tuberculum ventrale* is caudally protruding, but its articular surface is caudodorsally oriented. The *tuberculum dorsale* is oval, craniodistally elongated and caudally oriented. The *fossa pneumotricipitalis* is wide, shallow, and is caudodistally oriented. The *margo caudalis* is very marked in all its extension, which gives to the element a markedly triangular section, as in *F. ardesiaca*. The *crista deltopectoralies* is caudally oriented. The general morphology of this crest is similar to other members of *Fulica*, however, this structure does not preserve the proximal and distal vertices. As in *F. ardesiaca*, the cranial border of the *crista deltopectoralis* is relatively straight, while in *F. armillata* this border is concave. Furthermore, the dorsal surface of the *crista deltopectoralis* presents a marked longitudinal break, as in *Fulica ardesiaca*. In cranial view, the *sulcus ligamentus transversus* is dorsoventrally short and is restricted to the ventral margin of the proximal portion of the humerus, as in other species of *Fulica*. The *sulcus ligamentus transversus* is deep in its most cranioventral portion and becomes more superficial and proximodistally wide in its caudodorsal portion. As in other members of *Fulica*, the *impressio coracobrachialis* is very poorly excavated. Although several traits agree with the humerus of *F. ardesiaca*, some small morphological discrepancies hinder a more precise allocation.

Fulica sp. (Fig. 5P).

Referred material: A proximal portion of a left humerus (SGO.PV.23223).

Locality and horizon: TT-1 archaeo-paleontological site, Laguna de Tagua Tagua, late Pleistocene - early Holocene, O'Higgins region, Central Chile.

Description and comparisons: In the specimen SGO.PV.23223, the *caput humeri* is flattened and with a very porous texture (Fig. 5P). This porosity suggests that the humerus fragment belonged to an osteologically immature individual at the time of death (Tumarkin-Deratzian et al., 2006). Despite the fact that the element belongs to a young individual, it possesses a size and robustness greater than *F. rufifrons*, *F. ardesiaca* and *F. leucoptera*, being in the range of *F. armillata*. The specimen SGO.PV.23223 lacks a portion of the proximal *crus ventrale fossae section*. In *F. armillata*, the *crus ventral fossae* distally extends as a ventrally protruding rim until converges in the cranioventral ridge of the diaphysis, at the same level of the distal vertex of the *crista deltopectoralis*. On the contrary, in the specimen SGO.PV.23223 the *crus ventrale fossae* does not extend distally like a rim and does not reach the distal vertex of the *crista deltopectoralis*. The angle in which the distal portion of the *crista deltopectoralis* converges with the diaphysis is wider than in *F. armillata*. The *incisura capitis* is slightly less excavated than in *F. armillata*, and its distal end is proportionally wider than in that species. The *fossa pneumotricipitalis* is broad, shallow, and caudoventrally oriented. In the caudoventral surface, distally to the *fossa pneumotricipitalis*, there is a small nutritional foramen, which is located inside of a well-developed longitudinal sulcus. In *F. armillata* this foramen is smaller and located outside the longitudinal sulcus. The *crista deltopectoralis* is cranially protruding. The morphology of the *crista deltopectoralis* is similar to *F. armillata*. Its proximal edge is distally inclined until it converges with a distally curved hook-shaped edge. The cranial ridge of the *crista deltopectoralis* is proximally concave and parallel to the humerus longitudinal axis. Distally, the lateral edge of the *crista deltopectoralis* ends in another vertex, and then progressively approaches the

dorsal surface of the diaphysis until it converges with its surface. On the distal surface, the *sulcus ligamentus transversus* is dorsoventrally short and ventrally restricted. This groove is deeper ventrally than dorsally. As in reference material of *Fulica* material, the *impressio coracobrachialis* is very poorly excavated.

Genus *Pardirallus* Bonaparte (1856)

Pardirallus sanguinolentus Swainson (1138) (Fig. 5Q).

Referred material: A right humerus without the *caput humeri* (SGO. PV.23283).

Locality and horizon: TT-1 archaeo-paleontological site, Laguna de Tagua Tagua, late Pleistocene - early Holocene, O'Higgins region, Central Chile.

Description and comparisons: The specimen SGO.PV.23283 (Fig. 5Q) corresponds to a humerus of an adult individual of a small-sized rallid, in the size range of *F. rufifrons* and *P. sanguinolentus*. The *incisura capitis* is oval, proximodistally wide and is well excavated. The *tuberculum ventrale* is medially well developed, and its articular surface is dorsomedially oriented as in *P. sanguinolentus*. The *margo caudalis* is well developed, but to a lesser extent than in species of *Fulica*, such as *F. armillata*. The *fossa pneumotricipitalis* is rounded, wide, shallow, and is caudoventrally oriented. The diaphysis is tubular in its medial portion and triangular in its proximal one. Distally, the *processus flexorius* is distally projected, the *sulcus humerotricipitalis* is dorsomedially wide and shallow, while the *sulcus scapulotricipitalis.* is short and progressively deeper distally. In dorsal view, the *crista deltopectoralis* is morphologically similar to *Pardirallus sanguinolentus*, and to reference specimens of *Fulica*, such as *F. rufifrons* and *F. ardesiaca*. The *crista deltopectoralis* presents a caudally inclined proximal ridge, a proximal vertex, an anterior ridge parallel to the longitudinal axis of the bone, which is slightly concave, a distal arista, and an inclined distal ridge with respect to the diaphysis, which distally converges with it. In cranial view, the *impressio coracobrachialis* is deeper than in reference specimens of *Fulica*, but it agrees with *Pardirallus sanguinolentus*. The *condylus dorsalis* is oval in shape. Its longitudinal axis is medially inclined, and its proximal portion is medially curved. The *condylus ventralis* is proximally flattened and distally rounded and its longest axis is dorsoventrally oriented, forming an acute angle with the longitudinal axis of the *condylus dorsalis*. The *fossa musculi brachialis* is shallow, its medial section is dorsomedially wide, but it narrows proximally, and its longitudinal axis is medially inclined, as in *Pardirallus sanguinolentus*. The *tuberculum supracondylare ventrale* is cranially well developed, presents a flat surface cranially oriented, which is proximally narrow and distally wide. The *processus supracondylaris dorsalis* is dorsally protruding. The distal portion of the humerus is wide and the *epicondylus ventralis* is offset, as is described in *Pardirallus* (Zelenkov et al., 2017), whereas the *epicondylus dorsalis* is not well developed. The *processus flexorius* is distally protruding, as in several genera of rallids (Zelenkov et al., 2017).

Rallidae indet. (Fig. 5R-S).

Referred material: A proximal portion of a right humerus (SGO. PV.23284), and a proximal portion of a right humerus with almost all of its proximal portion absent (SGO.PV.23286).

Locality and horizon: TT-1 archaeo-paleontological site, Laguna de Tagua Tagua, late Pleistocene - early Holocene, O'Higgins region, Central Chile.

Description and comparisons: Both specimens belong to adult individuals, within the size range of *Fulica rufifrons*, *Fulica leucoptera* and *Pardirallus sanguinolentus* (Fig. 5R–S). The specimen SGO.PV.23284 lacks its proximoventral portion, so crucial structures such as *fossa pneumotricipitalis*, *tuberculum ventrale* and *incisura capitis* are absent (Fig. 5R). The *caput humeri* possesses a subtriangular contour in cranial and caudal view and is proximally rounded. The *tuberculum dorsale* is oval in shape and is caudodistally oriented. The *margo caudalis* is well developed which confers to the proximal portion of the diaphysis a triangular cross section. In dorsal view, the *crista deltopectoralis* is cranially well developed. The ridges of this feature are partially broken, making it impossible to define its exact shape, however, it resembles the

crista deltopectoralis of reference specimens of *Fulica*. In cranial view, the *impressio coracobrachialis* is shallower than in reference specimens of *Fulica*.

In turn, the specimen SGO.PV.23286 lacks most of its proximal portion (Fig. 5S). The *margo caudalis* is well developed, conferring it a triangular section in its proximal portion. In dorsal view, the *crista deltopectoralis* is cranially developed. Its contour is similar to reference specimens of *Fulica*, such as *F. armillata*. In these taxa, the proximal ridge of the *crista deltopectoralis* is distally inclined and presents a proximal and distal vertex which flanks the cranial ridge of the *crista deltopectoralis*. The latter is parallel to the axis of the specimen and is slightly concave. The distal ridge of the *crista deltopectoralis* progressively reaches the diaphysis towards distal, until converges with it. In cranial view, the *impressio coracobrachialis* is shallow.

5. Discussion

Rails have been traditionally considered osteologically conserved, making it difficult to segregate among different taxa (Taylor, 1996; Mayr and Smith, 2001). For example, the appendicular skeleton of the genera *Lewinia* and *Rallus* are very difficult to differentiate, with some bone elements such as the tibiotarsus, practically identical in both genera (Zelenkov et al., 2017). Olson (1974) in his review of the North American extinct rallids suggested a change in status of several taxa such as *Fulica hesterna* (Howard, 1963), *Laterallus guti* (Brodkorb, 1952) and *Epirallus natator* (Miller, 1942), mainly due to the difficulties in differentiating species based on the study of their bones. In Olson's opinion (1974) the remains used to describe *Fulica sterna* and *Laterallus guti* were insufficient or belonged to extant species. In addition, Olson (1974) synonymized the genus *Epirallus* with the genus *Rallus*. However, this author maintained the combination *Rallus natator* as valid, since the size of this species was greater than the extant species *Rallus elegans* and *Rallus longirostris*.

To cope with this difficulty, we presented here a detailed study of humeri, coracoids, tibiotarsi and tarsometatarsi from different South American extant species of rallids, which has allowed us to distinguish several consistent traits on each species. All of these traits were satisfactorily contrasted in the fossil sample as well.

Each of these features and elements has been used before to differentiate and diagnose rallid species (Zelenkov et al., 2017; Takano and Steadman, 2018; Mather et al., 2018). For example, the anatomy of the coracoid frequently allows the identification of taxa at the genus level (Zelenkov et al., 2017). Likewise, the tarsometatarsus is one of the most informative elements being useful for describing new species, since in most cases it is possible to distinguish features of diagnostic value. Among these informative features are the size and slenderness of the bone, the position of foramina along the same, and the morphology of the trochleae and hypotarsal ridges (Takano and Steadman, 2018; Mather et al., 2018). This was the case of *Fulica montanei*, in which the most diagnostic traits were in the proximal portion of the tarsometatarsus as well as in the trochleae. The size was also used for the diagnosis, since the tarsometatarsus of *F. montanei* is in the range of the extant *Fulica cornuta* and the extinct *Fulica prisca*, both considered "giant species''. At the same time is also bigger than the metatarsi of the extant coots that inhabit central Chile.

On the other hand, some of the bones in our fossil sample could not be satisfactorily assigned to the species level. This is the case of the proximal portion of the humerus referred to *Fulica* sp. (SGO.PV.23223). This bone belonged to an immature individual since the caput humeri was not yet ossified at the time of the death of the animal. The size of this specimen is in the range of *F. armillata*, which is the largest coot in central Chile at present (Couve et al., 2016; Martínez-Piña and González-Cifuentes, 2017). However, SGO.PV.23223 has some features that suggest it does not belong to this species: the humerus fragment is slightly more robust than the humerus of *F. armillata*, the capitis notch is wider and less excavated, and the *crus ventrale* fossae is poorly developed

distally. Although it is possible that this fragment of the humerus may belong to *F. montanei*, there is no robust evidence to support this at the moment. Besides the tarsometatarsus described here there are no more skeletal elements known for this new species at present.

Fulica montanei was stratigraphically associated with several rallid taxa. Among these, both *F. rufifrons* and *F. armillata* are coots that currently inhabit lacustrine and wetlands environments in central Chile (Couve et al., 2016; Martínez-Piña and González-Cifuentes, 2017). The presence of both *Fulica rufifrons* and *Fulica armillata* had previously been recorded in LTTF deposits from isolated appendicular elements (Alarcón et al., 2014, 2016; Labarca et al., 2020). These taxa currently coexist with the small *F. leucoptera*, a coot that has not been detected in the fossil record of LTTF so far. Interestingly, our results indicate the presence of *Fulica* cf. *F. ardesiaca*, which in present-day Chile inhabits lakes, cushion bogs and lagoons of the high mountain range, in the northern part of the country (~17°5′-27°S), although, can be found occasionally in low-altitude areas as well (Couve et al., 2016; Martínez-Piña and González-Cifuentes, 2017). There are isolated records further south for this species (Yury-Yáñez et al., 2009), being the southernmost report in the wetland of Batuco (33°2′S), about 150 km north of Laguna de Tagua Tagua (e-Bird, 2020). Given the current distribution of *F. ardesiaca*, it is possible to suggest that it corresponds to a remnant of a larger Holocene distribution, which could have been affected and reduced in geographic extension by anthropic and/or climatic factors. Finally, there is the identification in the LTTF of the small *P. sanguinolentus*, which currently lives in the study area (Couve et al., 2016).

The finding of an extinct giant coot in the LTTF, coexisting with three extant taxa that currently live in the area and with a locally extirpated taxa, indicates that the late Pleistocene - early Holocene rallid richness of central Chile was higher than today. These results are consistent with the generalized high richness of rallids during the late Quaternary reported in different parts of the world (Olson, 1977; Worthy, 2004) and also with the known high speciation rates of the family (García-R et al., 2014).

The remarkable length and robustness of the tarsometatarsi analyzed suggest that *F. montanei* was a heavy coot, probably in the range of *F. cornuta* and *F. prisca* (Table 1 and Fig. 4A and B). Both *F. cornuta* and *F. gigantea*, are the biggest extant coots in the world at present and exhibit a limited flying capability. The extinct New Zealand giant species *F. prisca* and *F. chathamensis* are also described as flightless birds (Livezey, 2003). Taking this information into account it is possible to infer a similar capacity for the Montane's coot, but unfortunately, the sparse fossil material recovered so far prevents a more detailed discussion about this topic (i.e. wing bone proportion with respect to body mass, lack of pneumaticity, etc). With regards to the ethology of *F. montanei*, the finding of the fossil materials in a lacustrine context suggests aquatic habits, as is the case for most of the members of the Rallidae. The presence of three left tarsometatarsi in the bone assemblage, representing three individuals, suggests that the species may have been relatively abundant in LTTF during the Pleistocene - Holocene transition. However, the difficulty of assigning other elements to this new species makes difficult to corroborate this hypothesis.

Montane's coot is the first well-documented extinct coot of the Quaternary of South America. As it was mentioned in the introduction, all the previous rallid fossils recorded for the continent have been referred to extant taxa. Campbell (1979) mentions the finding of appendicular elements of *Porzana carolina* Linnaeus in the Talara Tar Seeps (late Pleistocene), Piura Department, Peru. In Argentina, Tonni and Laza (1980) mentioned the presence of *Fulica leucoptera* in Paso Otero, Luján Formation (late Pleistocene), Buenos Aires Province, Argentina. Later, in the same locality, Cenizo et al. (2015) identified *Fulica leucoptera, Fulica rufifrons, Fulica* sp. cf. *F. leucoptera-F. rufifrons* and *Fulica* sp. cf. *F. armillata*. Vezzosi et al. (2010) reports several rallid bones found in deposits of the Ñuapua Formation (early Holocene), Bolivia, which are assigned to *Pardirallus* cf. *P. sanguinolentus, Gallinula chloropus, Gallinula* cf. *G. melanops* and *Fulica* cf. *F. rufifrons*, although

they do not provide descriptions of the elements on which those identifications are based. In turn, the type material of *Euryonotus brachypterus* and *Euryonotus argentinus* needs a revaluation, remaining both taxa as *nonima dubia* (Olson, 1977, 1981).

Our findings add new evidence to the practically non-existent rail record of continental Chile, which as far as we know includes two localities only. Humphrey et al., 1993, mentions the discovery of a distal portion of a left femur and the distal portion of a right tarsometatarsus in Fell's Cave, in southern Patagonia, which were identified as *F. armillata*. Cartajena (2002) reports *Fulica* sp., based on the description of an ulna, in the late Pleistocene - early Holocene archaeological site of Tuina 5, located in the altiplano of northern Chile. Additionally, Steadman (1985) mentions the existence of two extinct endemic rails found in a Holocene archaeological site from Rapa Nui, insular Chile. This record includes the presence of the genus *Porzana* and an undetermined rallid, however no detailed descriptions of the specimens studied are given in the publication.

So far no bones of Montane's coot have been documented in middle/late Holocene archaeological sites studied in LTTF (Jackson et al., 2012), suggesting this coot became extinct at the end of the Pleistocene or beginning of the Holocene, a time where the disappearance of mega-mammals is also recorded in the area (Núñez et al., 1994). The causes of the extinction of *F. montanei* remain unclear, however it could be linked to the dramatic climate change that characterized the Pleistocene - Holocene transition in the area of Laguna de Tagua Tagua (Heusser, 1990; Valero-Garcés et al., 2005). The impact of humans in this environment could be considered as well, since anthropogenic disturbance has provoked more rallid extinctions than any other avian family (Ripley, 1977; Steadman, 1995; Taylor, 1998; Hume, 2017), especially of flightless taxa that evolved in islands (Worthy, 2004; Hume, 2019). However, more robust and systematic evidence of rallid-human interactions would be necessary to sustain this hypothesis, which so far is absent in TT-1 and TT-2. At the moment, only evidence of anthropogenic exploitation of megafauna can be undoubtedly identified (Montané, 1968; Núñez et al., 1994; Labarca et al., 2020), nonetheless, a small-fauna hunting strategy could be expected as well, considering the high richness of birds, rodents and other small taxa documented in LTTF during late-glacial times (Casamiquela, 1976; Labarca et al., 2020). Small fauna exploitation, including birds, has been documented before in adjacent middle/late Holocene archaeological sites (Jackson et al., 2012). In sum, both alternatives must remain hypothetical, until more biostratigraphical, biogeographical and taphonomical research in LTTF and in nearby contemporaneous freshwater systems have been done.

6. Conclusions

Comparison of tarsometatarsi of extant coots and osteometric analyses, support the presence of a new species of giant coot that inhabited central Chile during the late Pleistocene - early Holocene. The unique combination of traits observed in these elements allows us to distinguish it as a new species which we have named here as *Fulica montanei*. Bivariate and multivariate analyses suggest that the size of *F. montanei* was similar to the extant *Fulica cornuta* and the extinct *Fulica prisca*, and clearly separated from the species that currently inhabit central Chile: *F. armillata, F. rufifrons* and *F. leucoptera*. These results make *F. montanei* the largest coot ever recorded in central Chile and the first extinct rallid well-documented in the Quaternary of South America. *F. montanei* coexisted with two coots and a rail that occur in central Chile at present, but also with a locally extirpated coot (*F. ardesiaca*) indicating a greater richness of the family Rallidae during late Pleistocene - early Holocene in the area. At the same time, Montane's coot coexisted with extinct megafauna (Gomphotheriidae, Cervidae, Equidae), as well as with small and medium-sized vertebrates (Didelphidae, Cricetidae, Abrocomidae, Octodontidae, Echimyidae, Canidae, Atherinopsidae, Calyptocephalellidae, Bufonidae, Dipsadidae, Anatidae, Columbidae, Podicipedidae, Accipitridae) and, presumably, with humans, constituting a

faunal assemblage with no analog today (Labarca et al., 2020). So far, the absence of middle and late Holocene records of *Fulica montanei* suggests that this taxon probably became extinct during the late Pleistocene-early Holocene.

Future research in Laguna de Tagua Tagua will probably provide more answers to questions related to the abundance of this species in the ecosystem, and the possible interactions that had with other species such as the first humans that inhabited central Chile at the end of the Pleistocene.

Nomenclatural acts

Species name: LSID:urn:lsid:zoobank.org:act:C267D560-58A8-45F4-ABDF-8037CFB1F0D6

Publication: LSID:urn:lsid:zoobank.org:pub:169E8479-232B-4EA5-8662-5CEBACF90997.

CRediT authorship contribution statement

Jhonatan Alarcón-Muñoz: Investigation, Writing - original draft, Conceptualization, Methodology, Visualization, Writing - review & editing. **Rafael Labarca:** Investigation, Conceptualization, Methodology, Formal analysis, Validation, Supervision, Visualization, Writing - review & editing, Funding acquisition. **Sergio Soto-Acuña:** Investigation, Validation, Writing - review & editing.

Declaration of competing interest

The authors declare that they have no known competing financial interests or personal relationships that could have appeared to influence the work reported in this paper.

Acknowledgements

References

Alarcón, J., Yury-Yáñez, R.E., Soto-Acuña, S., Rubilar-Rogers, D., Sallaberry, M., 2014. Las aves fósiles de la Laguna de Tagua Tagua (Pleistoceno Superior), Chile central. Ameghiniana 51 (6), R4.

Alarcón, J., 2016. Las aves fósiles de la Laguna de Tagua Tagua. Undergraduate thesis, Universidad de Chile, pp. 1–154.

Alcover, J.A., McMinn, M., Seghi, B., 2005. Fossil rails (Gruiformes: Rallidae) from the balearic islands. In: Alcover, J.A., Bover, P. (Eds.), Proceedings of the International Symposium "Insular Vertebrate Evolution: the Palaeontological Approach", 12. Monografies de la Societat d'Història Natural de les Balears, pp. 9–16.

Alvarenga, H.M.F., 1988. Ave fóssil (Gruiformes: Rallidae) dos folhelhos da Bacia de Taubaté, Estado de São Paulo, Brasil. Anais da Academia Brasileira de Ciências 60, 321–332.

Baumel, J.L., Witmer, L.M., 1993. Osteologia. In: Baumel, J.J., King, A.S., Breazile, J.E., Evans, H.E., Vanden Berge, J.C. (Eds.), Handbook of Avian Anatomy: Nomina Anatomica Avium. Nuttall Ornithological Club, Cambridge, pp. 45–132.

Boles, W.E., 2005. A new flightless gallinule (Aves: Rallidae: *Gallinula*) from the Oligo–Miocene of Riversleigh, northwestern Queensland, Australia. Records of the Australian Museum 57, 179–190. https://doi.org/10.2307/40168337.

Bonaparte, C.L., 1854. Conspectus systematicus ornithologiae. Annales des sciences naturelles/Zoologie 4, 105–152.

Bonaparte, C.L., 1856. Excursions dans les divers musées d'Allemagne, de Hollande et de Belgique (suite et fin), et tableaux paralléliques de l'ordre des Palmipèdes. Comptes Rendus Hebdomadaires des Séances de l'Académie des Sciences 43, 593–601.

Brodkorb, P., 1952. A new rail from the Pleistocene of Florida. The Wilson Bulletin 64, 80–82.

Campbell, K., 1979. The non-passerine Pleistocene avifauna of Talara taar Seeps, northwestern Perú. Life science contributions. Royal Ontario Museum 118, 1–203.

Cartajena, M.I., 2002. Los conjuntos arqueofaunísticos del Arcaico Temprano en la Puna de Atacama, Norte de Chile. Ph.D. Thesis, Freie Universität Berlin. ABESY Vertriebs GmbH.

Casamiquela, R.M., 1976. Los vertebrados fósiles de Tagua-Tagua. Actas del Primer Congreso Geológico Chileno, pp. C87–C102.

Cenizo, M.M., Agnolin, F.L., Pomi, L.H., 2015. A new Pleistocene bird assemblage from the Southern Pampas (Buenos Aires, Argentina). Palaeogeography, Palaeoclimatology, Palaeoecology 420, 65–81. https://doi.org/10.1016/j.palaeo.2014.12.009.

Clements, J.F., Schulenberg, T.S., Iliff, J., Sullivan, B.L., Wood, C.L., Roberson, D., 2012. The Clements checklist of birds of the world: version 6.7. Available from: http://www.birds.cornell.edu/clementschecklist/downloadable-clements-checklist. (Accessed 20 January 2020).

Couve, E., Vidal, C.F., Ruiz, J., 2016. Aves de Chile. Sus Islas Oceánicas y Península Antártica. Una guía de campo ilustrada. FS Editorial, Punta Arenas.

De Pietri, V.L., Mayr, G., 2014. Reappraisal of early Miocene rails (Aves, Rallidae) from central France: diversity and character evolution. Journal of Zoological Systematics and Evolutionary Research 52 (4), 311–322. https://doi.org/10.1111/jzs.12074.

E-bird, 2020. *Fulica ardesiaca*. the cornell laboratory of ornithology. Available from: https://ebird.org/species/slccoo1/. (Accessed 10 April 2020).

García-R, J.C, Gibb, G.C., Trewick, S.A., 2014. Deep global evolutionary radiation in birds: diversification and trait evolution in the cosmopolitan bird family Rallidae. Molecular Phylogenetics and Evolution 81, 96–108. https://doi.org/10.1016/j.ympev.2014.09.008.

García-R, .J.C., Lemmon, E.M., Lemmon, A.R., French, N., 2020. Phylogenomic Reconstruction Sheds Light on New Relationships and Timescale of Rails (aves: Rallidae) Evolution. Diversity 12 (2), 70. https://doi.org/10.3390/d12020070.

Gill, B.J., Bell, B.D., Chambers, G.K., Medway, D.G., Palma, R.L., Scofield, R.P., Tennyson, A.J.D., Worthy, T.H., 2010. Checklist of the Birds of New Zealand, Norfolk and Macquarie Islands, and the Ross Dependency, Antarctica, fourth ed. Ornithological Society of New Zealand & Te Papa Press, Wellington.

Heusser, C.J., 1983. Quaternary pollen record from Laguna de Tagua Tagua, Chile. Science 219, 1429–1432.

Heusser, C.J., 1990. Ice age vegetation and climate of subtropical Chile. Palaeogeography, Palaeoclimatology, Palaeoecology 80, 107–127.

Holdaway, R.N., Worthy, T.H., Tennyson, A.J.D., 2001. A working list of breeding bird species of the New Zealand region at first human contact. New Zealand Journal of Zoology 28, 119–187. https://doi.org/10.1080/03014223.2001.9518262.

Houde, P., 2009. Cranes, rails, and allies. In: Hedges, S.B., Kumar, S. (Eds.), The Timetree of Life. Oxford University Press, pp. 440–444.

Howard, H., 1963. Fossil birds from the Anza-Borrego desert. Los Angeles County Museum Contributions in Science 73, l–33.

Hume, J.P., 2017. Extinct Birds, Second ed. Helm, London.

Hume, J.P., 2019. Systematic, morphology and ecology of rails (Aves: Rallidae) of the Mascarene Islands, with one new species. Zootaxa 4626 (1), 1–107. https://doi.org/10.11646/zootaxa.4626.1.1.

Hume, J.P., Martill, D., 2019. Repeated evolution of flightlessness in *Dryolimnas* rails (Aves: Rallidae) after extinction and recolonization on Aldabra. Zoological Journal of the Linnean Society 186 (3), 666–672. https://doi.org/10.1093/zoolinnean/zlz018.

Humphrey, P.S., Pefaur, J.E., Rasmussen, P.C., 1993. Avifauna of three Holocene deposits of southern Chile. Occasional Papers of the Museum of Natural History. The University of Kansas, Lawrence, Kansas, p. 37.

Jackson, D., Aspillaga, E., Rodríguez, X.-P., Jackson, D., Santana, F., Méndez, C., 2012. Las Ocupaciones Humanas del Sitio Arqueológico de Santa Inés, Laguna de Tagua Tagua, Chile Central. Revista de Antropología 26, 151–168. https://doi.org/10.5354/0719-1472.2012.26558.

Kaiser, J., Lamy, F., Hebbeln, D., 2005. A 70-kyr sea surface temperature record of southern Chile (Ocean Drilling Program Site 1233). Paleoceanography 20 (4), PA4009. https://doi.org/10.1029/2005PA001146.

Kirchman, J.J., Steadman, D.W., 2005. Rails (Aves: Rallidae: *Gallirallus*) from prehistoric sites in the Kingdom of Tonga, including the description of a new species. Proceedings of the Biological Society of Washington 118, 465–477. https://doi.org/10.2988/0006-324X(2005)118[465:RARGFP]2.0.CO;2.

Kirchman, J.J., Steadman, D.W., 2007. New species of extinct rails (Aves: Rallidae) from archaeological sites in the Marquesas islands, French Polynesia. Pacific Science 61 (1), 145–163. https://doi.org/10.1353/psc.2007.0008.

Labarca, R., González-Guarda, E., Lizama-Catalán, Á., Villavicencio, N.A., Alarcón-Muñoz, J., Suazo-Lara, F., Oyanadel-Urbina, P., Soto-Huenchuman, P., Salazar, C., Soto-Acuña, S., Buldrini, K.E., 2020. Taguatagua 1: new insights into the late Pleistocene fauna, paleoenvironment, and human subsistence in a unique lacustrine context in central Chile. Quaternary Science Reviews 238, 106282 doi: 0.1016/j.quascirev.2020.106282.

Linnaeus, C., 1758. Systema Naturae per Regna Tria Naturae, secundum classes, ordines, genera, species, cum characteribus, differentiis, synonymis, lacis, , 10th1. Impensis Laurentii Salvii, Stockholm, pp. 1–823.

Livezey, B.C., 1998. A phylogenetic analysis of the Gruiformes (Aves) based on morphological characters, with an emphasis on the rails. Philosophical Transactions of the Royal Society of London B 353, 2077–2151. https://doi.org/10.1098/rstb.1998.0353.

Livezey, B.C., 2003. Evolution of flightlessness in rails (Gruiformes: Rallidae) phylogenetic, ecomorphological, and ontogenetic perspectives. Ornithological Monographs 53. https://doi.org/10.2307/40168337.

Livezey, B.C., Zusi, R.L., 2006. Higher-order phylogeny of modern birds (Theropoda, Aves: Neornithes) based on comparative anatomy: I —methods and characters. Bulletin of Carnegie Museum of Natural History 37, 1–544.

Martínez-Piña, D., González-Cifuentes, G., 2017. Las Aves de Chile. Guía de campo y Breve Historia Natural. Ediciones del Naturalista, Santiago, Chile.

Mather, E.K., Tennyson, A.J.D., Scofield, R.P., De Pietri, V.L., Hand, S.J., Archer, M., Handley, W.D., Worthy, T.H., 2018. Flightless rails (aves: Rallidae) from the early miocene st bathans fauna, otago. New Zealand Journal of Systematic Palaeontology 17 (5), 423–499. https://doi.org/10.1080/14772019.2018.1432710.

Mayr, G., Smith, R., 2001. Ducks, rails, and limicoline waders (aves: anseriformes, Gruiformes, charadriiformes) from the lowermost Oligocene of Belgium. Geobios 34 (5), 547–561. https://doi.org/10.1016/S0016-6995(01)80069-3.

Mayr, G., 2004. Phylogenetic relationships of the Early Tertiary messel rails (Aves, Messelornithidae). Senckenberg. Lethaea 84 (1/2), 317–322.

Mayr, G., 2015. Variations in the hypotarsus morphology of birds and their evolutionary significance. Acta Zoologica (Stockholm) 97, 196–210.

Mayr, G., 2019. Hypotarsus morphology of the Ralloidea supports a clade comprising *Sarothrura* and *Mentocrex* to the exclusion of *Canirallus*. Acta Ornithologica (Warszaw) 54, 51–58. https://doi.org/10.3161/00016454AO2019.54.1.005.

Mayr, G., Bochenski, Z.M., 2016. A skeleton of a small rail from the Rupelian of Poland adds to the diversity of early Oligocene Ralloidea. Neues Jahrbuch für Geologie und Paläontologie. Abhandlungen 282 (2), 125–134.

Mercerat, A., 1897. Note sur les oiseaux fossiles de la République Argentine. Anales de la Sociedad Científica Argentina 43, 222–240.

McMinn, M., Palmer, M., Alcover, J.A., 2005. A new species of rails (aves: Rallidae) from the upper Pleistocene and Holocene of Eivissa (Pityusic islands, western mediterrean). Ibis 147, 706–716. https://doi.org/10.1111/j.1474-919X.2005.00442.x.

Millner, L., 1942. Two New Bird Genera from the Pleistocene of Mexico. University of California Publications in Zoology, pp. 47343–47346.

Montané, J., 1968. Paleo-Indian remains from laguna de Tagua Tagua, Central Chile. Science 161 (3846), 1137–1138. https://doi.org/10.1126/science.161.3846.1137.

Mourer-Chauviré, C., 2000. A new species of *Ameriphodius* (Aves: Galliformes: Quercymegapodiidae) from the Lower Miocene of France. Paleontology 43 (3), 481–493.

Noriega, J.I., 1995. The avifauna from the "Mesopotamian" (Ituzaingó Formation: upper Miocene) of entre ríos Province, Argentina. Cour. Forschungsinst. Senckenberg 181, 141–148.

Noriega, J.I., Agnolin, F.L., 2008. El registro paleontológico de las Aves del "Mesopotamiense" (Formación Ituzaingó; Mioceno tardío-Plioceno) de la provincia de Entre Ríos, Argentina. INSUGEO, Miscelánea 17 (2), 271–290.

Núñez, L., Varela, J., Casamiquela, R., Schiappacasse, V., Niemeyer, H., Villagrán, C., 1994. Cuenca de Taguatagua en Chile: el ambiente del Pleistoceno superior y ocupaciones humanas. Revista Chilena de Historia Natural 67, 503–519.

Olson, S.L., 1973. A classification of the Rallidae. The Wilson Bulletin 85, 381–416.

Olson, S.L., 1974. The Pleistocene rails of north America. Condor 76, 169–175.

Olson, S.L., 1977. A synopsis on the fossil Rallidae. In: Ripley, D.S. (Ed.), Rails of the World: A Monograph of the Family Rallidae. Codline, Boston, pp. 339–389.

Olson, S.L., 1981. Natural history of vertebrates on the Brazilian islands of the mid south atlantic. National Geographic Society Research Reports 13, 481–492.

Philippi, R.A., Landbeck, L., 1861. Sobre las especies chilenas del jénero *Tulica* (sic). Anales de la Universidad de Chile 19, 501–510.

Rafinesque, C.S., 1815. Analyse de la nature, ou tableau de l'univers et des corps organisés. Published by the author, Palermo, 1–224.

Ripley, S.D., 1977. Rails of the World: a Monograph of the Family Rallidae. David R. Godine Publisher.

Steadman, D.W., 1995. Prehistoric extinctions of Pacific Island birds: biodiversity meets zooarchaeology. Science 267, 1123–1131. https://doi.org/10.1126/science.267.5201.1123.

Swainson, W., 1838. Animals in Menageries. Printed for Longman, Orme, Brown, Green & Longmans, and John Taylor, London, pp. 1–373.

Takano, O.M., Steadman, D.W., 2018. Another new species of flightless rail (Aves: Rallidae: *Rallus*) from Abaco, the Bahamas. Zootaxa 4407 (3), 376–382. https://doi.org/10.11646/zootaxa.4407.3.5.

Tambussi, C., Degrange, F., 2013. South American and Antarctic continental Cenozoic birds: Paleobiogeographic affinities and disparities. Springer, Dordrecht and London, 1–114.

Taylor, P.B., 1996. Family Rallidae (rails, gallinules and coots). Hoatzin to Auks. In: del Hoyo, J., Elliot, A., Sargatal, J. (Eds.), Handbook of the Birds of the World, vol. 3. Lynx Edicions, Barcelona, pp. 108–209.

Taylor, P.B., 1998. Rails: a Guide to the Rails, Crakes, Gallinules and Coots of the World. Pica Press, Robertsbridge.

Taylor, P.B., 2010. Rails: a Guide to Rails, Crakes, Gallinules and Coots of the World. Bloomsbury Publishing, London.

Tschudi, J.J.v., 1843. Diagnosen einiger neuer peruanischen Vögel. Archiv für Naturgeschichte 9, 385–390.

Tumarkin-Deratzian, A.R., Vann, D.R., Dodson, P., 2006. Bone surface texture as an ontogenetic indicator in long bones of the Canada goose *Branta canadensis* (Anseriformes: Anatidae). Zoological Journal of the Linnean Society 148, 133–168.

Tonni, E.P., Laza, J.H., 1980. Las aves de la Fauna local Paso Otero (Pleistoceno Tardío) de la provincia de Buenos Aires. Su significación ecológica, climática y zoogeográfica. Ameghiniana 17, 313–322.

Valero-Garcés, B.L., Jenny, B., Rondanelli, M., Delgado Huertas, A., Burns, S.J., Veit, H., Moreno, A., 2005. Palaeohydrology of Laguna de Tagua Tagua (34° 30′ S) and moisture fluctuations in Central Chile for the last 46 000 yr. Journal of Quaternary Science 20 (7-8), 625–641. https://doi.org/10.1002/jqs.988.

Varela, J., 1976. Estudio Estratigráfico-Sedimentológico de los depósitos de Laguna de Tagua Tagua, Provincia de O'Higgins. Undergraduate Thesis, Universidad de Chile.

Vezzosi, R.I., Brunetto, E., Noriega, J.I., 2010. Las Aves de la Formación Ñuapua (Holoceno temprano) de Bolivia. Ameghiniana 47 (1), 123–128.

Vieillot, L.J.P., 1817. Le Pitpit a front blanc, *Sylvia albifrons*. Nouveau Dictionnaire d'Histoire Naturelle, , Nouvelle Édition11. Sève, J.E., Chez Deterville, Paris, pp. 1–276.

Vigors, N.A., 1825. XXII. Observations on the Natural Affinities that connect the Orders and Families of Birds. Transactions of the Linnean Society of London 14, 395–517.

Von den Driesch, A., 1976. A Guide to Measurement of Animal Bones from Archaeological Sites, vol. 1. Peabody Museum Bulletin, Cambridge, MA (Harvard Peabody Museum of Archaeology and Ethnology).

Wetmore, A., 1924. Fossil birds from south eastern Arizona. Proceedings of the United States National Museum 64 (2495), 1–18.

Winkler, D.W., Billerman, S.M., Lovette, I.J., 2020. Rails, gallinules, and coots (Rallidae), version 1.0. In: Billerman, S.M., Keeney, B.K., Rodewald, P.G., Schulenberg, T.S. (Eds.), Birds of the World. Cornell Lab of Ornithology, Ithaca. https://doi.org/10.2173/bow.rallid1.01.

Worthy, T.H., 2004. The fossil rails (Aves: Rallidae) of Fiji with descriptions of a new genus and species. Journal of the Royal Society of New Zealand 34, 295–314. https://doi.org/10.1080/03014223.2004.9517768.

Worthy, T.H., Boles, W.E., 2011. *Austrorallus*, a new genus of *Gallinula disneyi* (aves: Rallidae) and a description of a new species from Oligo-Miocene deposits at Riversleigh, northwestern Queensland, Australia. Record Aust. Mus. 63, 61–77. https://doi.org/10.3853/j.0067-1975.63.2011.1563.

Yury-Yáñez, R., Torres-Araneda, A., Soto-Acuña, S., 2009. New observations of *Fulica ardesiaca* (Gruiformes: Rallidae) from Carrizal Bajo wetlands and a possible case of hybridization, 58. Boletín del Museo Nacional de Historia Natural, pp. 100–103.

Zelenkov, N.V., Panteleyev, A.V., De Pietri, V.L., 2017. Late miocene rails (Aves: Rallidae) from southwestern Russia. Palaeobiodiversity Palaeoenvironments 97, 791–805. https://doi.org/10.1007/s12549-017-0276-1.